Entanglement asymmetry in CFT and its relation to non-topological defects

Michele Fossati [ORCID],[a] Filiberto Ares [ORCID],[a] Jérôme Dubail [ORCID][b,c] and Pasquale Calabrese[a,d]

[a]*SISSA and INFN,*
  Via Bonomea 265, 34136 Trieste, Italy
[b]*CESQ and ISIS, CNRS & University of Strasbourg, UMR 7006,*
  67000 Strasbourg, France
[c]*LPCT, CNRS & Université de Lorraine, UMR 7019,*
  54000 Nancy, France
[d]*ICTP,*
  Strada Costiera 11, 34151 Trieste, Italy

  E-mail: mfossati@sissa.it

ABSTRACT: The entanglement asymmetry is an information based observable that quantifies the degree of symmetry breaking in a region of an extended quantum system. We investigate this measure in the ground state of one dimensional critical systems described by a CFT. Employing the correspondence between global symmetries and defects, the analysis of the entanglement asymmetry can be formulated in terms of partition functions on Riemann surfaces with multiple non-topological defect lines inserted at their branch cuts. For large subsystems, these partition functions are determined by the scaling dimension of the defects. This leads to our first main observation: at criticality, the entanglement asymmetry acquires a subleading contribution scaling as $\log \ell / \ell$ for large subsystem length ℓ. Then, as an illustrative example, we consider the XY spin chain, which has a critical line described by the massless Majorana fermion theory and explicitly breaks the U(1) symmetry associated with rotations about the z-axis. In this situation the corresponding defect is marginal. Leveraging conformal invariance, we relate the scaling dimension of these defects to the ground state energy of the massless Majorana fermion on a circle with equally-spaced point defects. We exploit this mapping to derive our second main result: the exact expression for the scaling dimension associated with n defects of arbitrary strengths. Our result generalizes a known formula for the $n = 1$ case derived in several previous works. We then use this exact scaling dimension to derive our third main result: the exact prefactor of the $\log \ell / \ell$ term in the asymmetry of the critical XY chain.

Contents

---

1 Introduction

Symmetries play a pivotal role in the foundations of modern physics. Their presence implies conservation laws that have deep consequences in the behavior of physical systems and facilitate enormously the resolution of many problems, which would otherwise remain open. As crucial as the existence of symmetries is their breaking, both explicit and spontaneous. Such breaking is responsible for a plethora of very important phenomena across different branches of physics. A relevant aspect that has received little attention so far is the quantification of how much a global symmetry is broken. Local order parameters have been usually employed to discern whether or not a quantum state respects a symmetry. However, they present the disadvantage that, while a non-zero value manifests that the symmetry is broken, the converse is not always true. Furthermore, in extended quantum systems, the question of measuring symmetry breaking is intrinsically tied to consider a specific subsystem. In fact, there may exist long-range correlations between the parts of the system that do not respect the symmetry and are not taken into account by any local order parameter.

In this context, an appealing idea is quantifying symmetry breaking by leveraging tools from the theory of entanglement, as they capture non-local correlations. A quantity based on the entanglement entropy and dubbed entanglement asymmetry has been recently introduced as a measure of how much a symmetry is broken in a subsystem. The entanglement asymmetry has proven to be a powerful instrument to identify novel physical phenomena. It has been applied to investigate the dynamical restoration of a U(1) symmetry from an initial state that breaks it after a quench to a Hamiltonian that respects the symmetry [1]. Surprisingly, the entanglement asymmetry shows that the restoration of the symmetry may occur earlier for those states that initially break it more, a quantum version of the yet unexplained Mpemba effect (the more a system is out of equilibrium, the faster it relaxes). This quantum Mpemba effect has been observed experimentally by measuring the entanglement asymmetry in an ion trap [2] and the microscopic mechanism and the conditions under which it occurs are now well understood for free and interacting integrable systems [3–5], although they remain elusive for non-integrable ones. In addition, the entanglement asymmetry has been applied to examine the dynamical restoration of a spontaneously broken $\mathbb{Z}_2$ symmetry [6] and the relaxation to a non-Abelian Generalized Gibbs ensemble in the exotic case that the symmetry is not restored [7]. It has been also generalized to study the quench dynamics of kinks [8]. Beyond non-equilibrium physics, the entanglement asymmetry has been employed to understand the implications of quantum unitarity for broken symmetries during black hole evaporation [9].

A significant point in the characterization of the entanglement asymmetry is its asymptotic behavior with the size of the subsystem considered. As this observable is based on the entanglement entropy, one may wonder whether it inherits some of its properties. For example, the entanglement entropy follows an area law in the ground state of one dimensional systems with mass gap. In contrast it grows logarithmically with the subsystem size when the mass gap vanishes; this logarithmic growth is proportional to the central charge of the conformal field theory (CFT) that describes the low energy physics of the critical point [10–12]. Conversely, the entanglement asymmetry exhibits a fundamentally distinct behavior. It has been shown in ref. [13] that, for matrix product states, the entanglement asymmetry for a generic compact Lie group grows at leading order logarithmically with the subsystem size, with a coefficient proportional to the dimension of the Lie group, while, for finite discrete groups, the entanglement asymmetry satisfies an area law, saturating to a value fixed by the cardinality of the group. Similar results have been obtained in the ground state of the XY spin chain when studying the particle number U(1) symmetry that this model explicitly breaks [4] and the spin-flip $\mathbb{Z}_2$ symmetry, spontaneously broken in the ferromagnetic phase [6, 14].

In this paper, we examine the implications of quantum criticality for the entanglement asymmetry, which remain barely unexplored, using CFT methods. Only ref. [15] reports calculations for the entanglement asymmetry in certain particular excited states of the massless compact boson. To this end, we develop a general scheme to compute the entanglement asymmetry in (1+1)-dimensional quantum field theories in terms of the charged moments of the subsystem's reduced density matrix. Employing the path integral formulation, the charged moments can be identified with the partition functions of the theory on Riemann surfaces with defect lines inserted along its branch cuts. These defect lines are associated with the elements of the symmetry group under analysis [16, 17]. A symmetry is considered broken

when the associated defects are not topological, and any continuous deformation of these defects leads to a change in the partition function. Therefore, within this framework, the entanglement asymmetry can be naturally interpreted as a measure of how much the defects are not topological. We apply this approach to determine the entanglement asymmetry in the ground state of the XY spin chain at the Ising critical line for the U(1) group of spin rotations around the transverse direction. After fermionizing it through a Jordan-Wigner transformation, the scaling limit of this model is described by the massless Majorana fermion theory and the defect lines corresponding to this group are marginal. We then exploit conformal invariance to map the Riemann surfaces to a single cylinder with defect lines parallel to its axis. In this setup, the calculation of the partition functions for large subsystems boils down to computing the ground state energy of the massless Majorana fermion on a circle with equally-spaced marginal point defects. The spectrum of this theory has been studied on the lattice in refs. [18, 19]. Here we revisit this problem and diagonalize systematically its Hamiltonian for an arbitrary number of equi-spaced point defects of different strengths. The study of defects in the massless Majorana fermion and Ising CFTs has a long story, see e.g. [16, 20–31]. Partition functions on Riemann surfaces with (topological and non topological) defect lines also arise in the analysis of the entanglement across inhomogeneities, interfaces, or junctions and after measurements [32–46]; in particular, those with topological defect lines appear in the symmetry resolution of entanglement measures [47–69], which has recently been investigated in profusion.

The paper is organized as follows. In section 2, we review the relation between symmetries and defects in (1+1)-quantum field theories, we introduce the entanglement asymmetry, and we show how to compute it from the partition function on a Riemann surface with defect lines. We also derive the asymptotic behavior of the entanglement asymmetry for a generic compact Lie group in the ground state of a one dimensional critical system. In the rest of the sections, we focus on the critical XY spin chain and the associated CFT, the massless Majorana fermion theory. In section 3, we introduce these systems and we review the known previous results for the entanglement asymmetry. In section 4, we calculate the partition function of the Majorana CFT on the Riemann surfaces that enter in the calculation of the entanglement asymmetry. In particular, by conformal invariance, these partition functions are given by the ground state energy of a massless Majorana fermion with evenly-spaced point defects. We carefully diagonalize its Hamiltonian for an arbitrary number of defects with different strengths. In section 5, we apply these results to obtain the entanglement asymmetry of the critical XY spin chain, checking them against exact numerical computations on the lattice. Finally, in section 6, we draw our conclusions and consider future prospects. We also include several appendices where we discuss with more detail some technical points of the main text.

2 Symmetries, topological defects, and entanglement asymmetry

In this section, we briefly review the identification between symmetries and topological defects. Then we introduce the Rényi entanglement asymmetry as a quantifier of symmetry breaking and we interpret it in terms of defects. With simple scaling arguments, we derive some general results for the asymptotic behavior of the Rényi entanglement asymmetry in the ground state of a critical one dimensional quantum system in the thermodynamic limit.
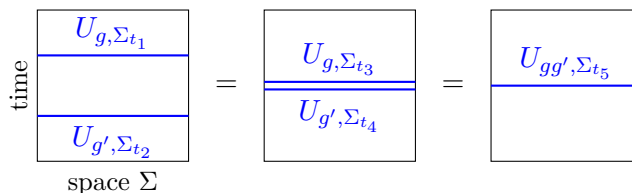
Figure 1. Each element g of a group G acts on the Hilbert space of an extended quantum system as a unitary operator $U_{\Sigma_t,g}$ defined along a line Σ_t at a fixed time t. If G is a symmetry of the theory, then any continuous transformation of Σ_t, as the ones performed in the figure, leaves invariant the partition function with insertions of these operators. We indicate this by the symbol = between the three diagrams. When two operators $U_{\Sigma_t,g}$ and $U_{\Sigma_t,g'}$ overlap, as in the right diagram, they can be fused according to the composition rule $U_{\Sigma_t,g}U_{\Sigma,g'} = U_{\Sigma_t,gg'}$.

2.1 Symmetries and topological defects

Global symmetries in spatially extended quantum systems are realized through extended operators that form a unitary representation of the symmetry group. In fact, if we consider a generic $(1+1)$-dimensional quantum field theory whose spacetime is a flat surface $\mathcal{M}$, then the action of an element g of the group G (either discrete or continuous) is implemented in its Hilbert space $\mathcal{H}$ by a unitary operator $U_{\Sigma_t,g}$ that has support on a spatial line $\Sigma_t \subset \mathcal{M}$ at a fixed time t. A familiar instance is the case of a U(1) symmetry. The Noether theorem ensures the existence of a conserved current j^μ. Therefore, the associated charge at Σ_t is $Q_{\Sigma_t} = \int_{\Sigma_t} dx\, j^0(x)$ and the group is represented by the operators $U_{\Sigma_t,\alpha} = \exp[i\alpha Q_{\Sigma_t}]$, with $\alpha \in [0, 2\pi)$.

The extended operators $U_{\Sigma_t,g}$ representing symmetries possess the crucial property of being *topological*. This means that continuous deformations of Σ_t do not affect any expectation value that contains the insertion of an operator $U_{\Sigma_t,g}$. For example, since a symmetry operator commutes with the Hamiltonian of the theory, it will not evolve in the Heisenberg picture and then $U_{\Sigma_t,g} = U_{\Sigma_{t'},g}$, as depicted in the first equality of figure 1. When the support of two extended operators $U_{\Sigma_t,g}$, $U_{\Sigma_t,g'}$ coincides, the operators fuse according to the standard composition rule $U_{\Sigma_t,g}U_{\Sigma_t,g'} = U_{\Sigma_t,gg'}$, as we illustrate in the second equality of figure 1.

The transformation of a field ϕ of the theory under the group G is described by a matrix R_g such that

$$U_{\Sigma_t,g}^\dagger \phi(x) U_{\Sigma_t,g} = R_g \phi(x), \quad x \in \Sigma_t. \tag{2.1}$$

Therefore, within the path integral formalism, the insertion of an operator $U_{\Sigma_t,g}$ in an expectation value is equivalent to performing a cut along the line Σ_t and imposing for the fields the following gluing conditions

$$\phi(x^+) = R_g \phi(x^-), \quad x \in \Sigma_t, \tag{2.2}$$

where $\phi(x^\pm)$ denote the field $\phi(x)$ at each side of the cut as we indicate in figure 2. The composition property $U_{\Sigma_t,g}U_{\Sigma_t,g'} = U_{\Sigma_t,gg'}$ can be then understood as the fusion of two cuts with gluing conditions R_g and $R_{g'}$ into a cut with gluing condition $R_g R_{g'} = R_{gg'}$. In Euclidean spacetime, $U_{\Sigma,g}$ is not needed to be defined along a line Σ_t orthogonal to the time

$$U_{\Sigma,g} \; \overline{} \overset{\bullet}{\underset{R_g\phi(x^-)}{}} \; = \; \overset{\phi(x^+)}{\underset{\bullet}{}} \overline{} \; U_{\Sigma,g}$$

Figure 2. Graphical representation of eq. (2.2). The insertion of an extended operator $U_{\Sigma,g}$ associated with the element g of a group G and with support on the line Σ corresponds, in the path integral approach, to a defect line along Σ with the gluing condition (2.2) for the field $\phi(x)$ at each side of the defect.

direction, but it can have support on any curve Σ on the surface $\mathcal{M}$. Due to the previous considerations, the extended operators $U_{\Sigma,g}$ are commonly referred to as *defects*, and when they enforce symmetries, they are *topological defects* [17]. A more detailed introduction to the role of topological operators in quantum systems can be found in, e.g., the recent review [70].

The question of whether a system is symmetric under a certain group can thus be reformulated as asking whether the defects associated to the symmetry are topological. In this paper, we are interested in quantifying the extent to which a symmetry is broken or, in other words, measuring how much the corresponding defects are not topological. This can be done with the entanglement asymmetry, which we now introduce.

2.2 Entanglement asymmetry

2.2.1 Definition

Let us take an extended quantum system in a state described by the density matrix ρ. We consider a spatial bipartition $\Sigma = A \cup \bar{A}$ in which A consists of a single connected region such that the total Hilbert space $\mathcal{H}$ factorizes into $\mathcal{H} = \mathcal{H}_A \otimes \mathcal{H}_{\bar{A}}$. We assume that the extended operators that represent the group G decompose accordingly as $U_{\Sigma,g} = U_{A,g} \otimes U_{\bar{A},g}$. The state of subsystem A is given by the reduced density matrix $\rho_A = \mathrm{tr}_{\bar{A}}\, \rho$, obtained by tracing out the degrees of freedom in the region $\bar{A}$. Under an element of the group G, it transforms as $\rho_A \mapsto U_{A,g}\rho_A U_{A,g}^\dagger$. Therefore, the state ρ_A is symmetric if $[\rho_A, U_{A,g}] = 0$ for all $g \in G$.

To define the entanglement asymmetry, we introduce the *symmetrization* of ρ_A as the average over G of the transformed density matrix $U_{A,g}\rho_A U_{A,g}^\dagger$; that is,

$$\rho_{A,G} := \frac{1}{\mathrm{vol}\,G} \int_G \mathrm{d}g\, U_{A,g}\rho_A U_{A,g}^\dagger, \tag{2.3}$$

if G is a compact Lie group, where $\mathrm{d}g$ is its Haar measure and $\mathrm{vol}\,G$ its volume. An analogous formula can be written up for a finite discrete group G of cardinality $|G|$ replacing the Haar integral by a sum over its elements. To lighten the discussion, we focus on compact Lie groups and we refer the reader to refs. [6, 13, 14] where the entanglement asymmetry has been examined for discrete groups. The density matrix $\rho_{A,G}$ is by construction symmetric under G and has trace one. Note that ρ_A is symmetric if and only if $\rho_A = \rho_{A,G}$. Then the entanglement asymmetry is the relative entropy between ρ_A an $\rho_{A,G}$ [1],

$$\Delta S_A := S(\rho_A || \rho_{A,G}) = \mathrm{tr}\left[\rho_A(\log \rho_A - \log \rho_{A,G})\right]. \tag{2.4}$$

Given the form of $\rho_{A,G}$, and applying the cyclic property of the trace, ΔS_A can be rewritten as

$$\Delta S_A = S(\rho_{A,G}) - S(\rho_A), \tag{2.5}$$
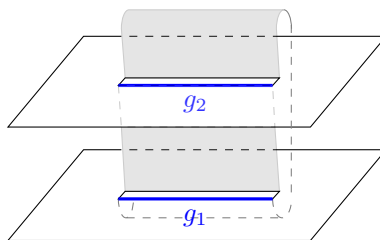
Figure 3. Riemann surface $\mathcal{M}_n$ for $n = 2$ (two sheets) with line defects (in blue) inserted along the branch cut of each sheet. The defects are associated respectively with the group elements g_1 and g_2. The quotient (2.12) of the partition functions on this surface with and without the line defects gives the normalized charged moment $\mathcal{Z}_2(\mathbf{g})$, defined in eq. (2.9). The Dirac delta in eq. (2.8) will set $g_2 = g_1^{-1}$.

where $S(\rho)$ is the von Neumann entropy of ρ, $S(\rho) = -\operatorname{tr}(\rho \log \rho)$. The entanglement asymmetry satisfies two essential properties as a measure of symmetry breaking in the subsystem A: it is non-negative, $\Delta S_A \geq 0$, and it vanishes if and only if A is in a symmetric state, i.e. $\rho_A = \rho_{A,G}$ [71, 72].

In general, the direct calculation of the entanglement asymmetry is complicated due to the presence of the logarithm in the von Neumann entropy. Alternatively, a much simpler indirect way of computing it is via the replica trick [10–12]. By replacing in eq. (2.5) the von Neumann entropy by the Rényi entropy, $S^{(n)}(\rho) = \frac{1}{1-n} \log \operatorname{tr} \rho^n$, we introduce the Rényi entanglement asymmetry

$$\Delta S_A^{(n)} = S^{(n)}(\rho_{A,G}) - S^{(n)}(\rho_A). \tag{2.6}$$

Observe that the entanglement asymmetry (2.5) is recovered in the limit $\lim_{n \to 1} \Delta S_A^{(n)} = \Delta S_A$. The advantage of the Rényi entanglement asymmetry is that, for integer n, it can be expressed in terms of charged partition functions. If we plug the definition of $\rho_{A,G}$ in eq. (2.6), we obtain

$$\Delta S_A^{(n)} = \frac{1}{1-n} \log \left[\frac{1}{(\operatorname{vol} G)^n} \int_{G^n} \mathrm{d}\mathbf{g} \frac{\operatorname{tr}(U_{A,g_1} \rho_A U_{A,g_1^{-1}} \dots U_{A,g_n} \rho_A U_{A,g_n^{-1}})}{\operatorname{tr}(\rho_A^n)} \right], \tag{2.7}$$

where $G^n = G \times \overset{n}{\dots} \times G$ and $\mathbf{g}$ stands for the n-tuple $\mathbf{g} = (g_1, \dots, g_n) \in G^n$. This integral can be rewritten as

$$\Delta S_A^{(n)} = \frac{1}{1-n} \log \left[\frac{1}{(\operatorname{vol} G)^{n-1}} \int_{G^n} \mathrm{d}\mathbf{g} \, \mathcal{Z}_n(\mathbf{g}) \delta \left(\prod_{j=1}^n g_j \right) \right], \tag{2.8}$$

where $\mathcal{Z}_n(\mathbf{g})$ are the (normalized) charged moments of ρ_A

$$\mathcal{Z}_n(\mathbf{g}) = \frac{\operatorname{tr}(\rho_A U_{A,g_1} \dots \rho_A U_{A,g_n})}{\operatorname{tr}(\rho_A^n)}. \tag{2.9}$$

2.2.2 Interpretation in terms of defects

In a (1+1) quantum field theory, using the path integral representation of the reduced density matrix ρ_A, the neutral moments $\operatorname{tr}(\rho_A^n)$ can be identified with the partition function on an

n-sheet Riemann surface $\mathcal{M}_n$ [11]. If we consider the ground state $|0\rangle$ of the theory, i.e. $\rho = |0\rangle\langle 0|$, and a single interval of length ℓ as subsystem A, the surface $\mathcal{M}_n$ is constructed as follows. We take the spacetime $\mathcal{M}$ where the theory is defined, which is the complex plane when working in Euclidean time and in the thermodynamic limit (infinite spatial direction). To obtain $\mathcal{M}_n$, we perform a cut on $\mathcal{M}$ along the interval $A = [0, \ell]$, we replicate n times this cut plane, and we sew the copies together along the cuts in a cyclical way, as we show in figure 3 for $n = 2$. Denoting as $Z(\mathcal{M}_n)$ the partition function on this surface, the neutral moments of ρ_A are given by

$$\text{tr}(\rho_A^n) = \frac{Z(\mathcal{M}_n)}{Z(\mathcal{M})^n}. \tag{2.10}$$

Following the discussion in section 2.1, the insertion of the operators U_{A,g_j} in this trace, as in eq. (2.9), corresponds to putting a defect line along the branch cut $[0, \ell]$ of each sheet of $\mathcal{M}_n$ with a gluing condition (2.2), being $g = g_j$, as depicted in figure 3. If $Z(\mathcal{M}_n^{\mathbf{g}})$ stands for the partition function on the surface $\mathcal{M}_n$ with these n defect lines, then we have that

$$\text{tr}(\rho_A U_{A,g_1} \cdots \rho_A U_{A,g_n}) = \frac{Z(\mathcal{M}_n^{\mathbf{g}})}{Z(\mathcal{M})^n}. \tag{2.11}$$

Therefore, in the ground state, the normalized charged moments $\mathcal{Z}_n(\mathbf{g})$ introduced in eq. (2.9) are the ratio of the partition functions on the surface $\mathcal{M}_n$ with and without n defect lines inserted at the branch cut of each sheet,

$$\mathcal{Z}_n(\mathbf{g}) = \frac{Z(\mathcal{M}_n^{\mathbf{g}})}{Z(\mathcal{M}_n)}. \tag{2.12}$$

If ρ_A is symmetric under G, then $[\rho_A, U_{A,g}] = 0$ for all $g \in G$. As we have previously seen, this implies that the defect lines associated with the insertions U_{A,g_j} are topological and they can be moved between the sheets of $\mathcal{M}_n$ under continuous transformations leaving the partition function $Z(\mathcal{M}_n^{\mathbf{g}})$ invariant. In that case, it is possible to fuse them in the same sheet, which is equivalent to the equality $\text{tr}(\rho_A U_{A,g_1} \ldots \rho_A U_{A,g_n}) = \text{tr}(\rho_A^n U_{A,g_1 \cdots g_n})$. Since the Dirac delta in (2.8) forces the product of all the group elements g_j to be the identity, the fusion yields $U_{A,g_1,\ldots g_n} = \mathbb{1}$. Consequently, $\mathcal{Z}_n(\mathbf{g}) = 1$ and, according to eq. (2.8), the Rényi entanglement asymmetry vanishes. On the other hand, if ρ_A is not symmetric, $[\rho_A, U_{A,g}] \neq 0$, then the defect lines associated to U_{A,g_j} are not topological. In that case, any continuous deformation of them does change the partition function $Z(\mathcal{M}_n^{\mathbf{g}})$ and, as a result, $\mathcal{Z}_n(\mathbf{g}) \neq 1$. In this sense, the *entanglement asymmetry quantifies how much the defect lines associated with a group are non topological*.

From generic scaling arguments, we can determine the asymptotic behavior of the partition functions $Z(\mathcal{M}_n)$ and $Z(\mathcal{M}_n^{\mathbf{g}})$. In two dimensions, the leading order contributions to the free energy $-\log Z$ are proportional to the area $|\mathcal{M}_n|$ of the surface $\mathcal{M}_n$, on which the partition function Z is defined. [Of course, strictly speaking, the area $|\mathcal{M}_n|$ is infinity, but it can be regularized, for instance by imposing periodic boundary conditions both spatial and imaginary time directions for each sheet of $\mathcal{M}_n$, far away from the interval.] Therefore, in the absence of defects,

$$-\log Z(\mathcal{M}_n) = f_{\text{bulk}} |\mathcal{M}_n| + O(1), \tag{2.13}$$

where f_{bulk} is the bulk free energy density. In the presence of defects, we expect that each of them contributes with an additional term proportional to the volume of the defect, which in this case is the length ℓ of the interval A. The free energy in that case is

$$-\log Z(\mathcal{M}_n^{\mathbf{g}}) = f_{\text{bulk}}|\mathcal{M}_n| + T_n(\mathbf{g})\ell + O(1), \quad \text{with} \quad T_n(\mathbf{g}) := \sum_{j=1}^{n} t(g_j), \qquad (2.14)$$

and $t(g_j)$ can be interpreted as the line tension of the defect associated with the insertion U_{A,g_j}. All these terms are cut-off dependent and, therefore, non universal. Plugging eqs. (2.13)–(2.14) into eq. (2.12), one sees that the bulk contribution in the free energy cancels, and the charged moments $\mathcal{Z}_n(\mathbf{g})$ decay exponentially with the subsystem length ℓ as

$$\mathcal{Z}_n(\mathbf{g}) = e^{-T_n(\mathbf{g})\ell + O(1)}. \qquad (2.15)$$

If the theory is critical, the conical singularities at the branch points of the surface $\mathcal{M}_n$ give rise in eqs. (2.13) and (2.14) to an extra universal (cut-off independent) term,

$$-\log Z(\mathcal{M}_n^{\mathbf{g}}) = f_{\text{bulk}}|\mathcal{M}_n| + T_n(\mathbf{g})\ell - \log Z_{\text{CFT}}(\mathcal{M}_n^{\mathbf{g}}) + O(1), \qquad (2.16)$$

which, as argued for instance in ref. [73], behaves as $-\log Z_{\text{CFT}}(\mathcal{M}_n^{\mathbf{g}}) \propto \log \ell$. The presence of defect lines may in general modify the coefficient of this term, so

$$\frac{Z_{\text{CFT}}(\mathcal{M}_n^{\mathbf{g}})}{Z_{\text{CFT}}(\mathcal{M}_n)} = \ell^{-\beta_n(\mathbf{g})} \qquad (2.17)$$

and it does not cancel in the ratio (2.12) of partition functions that gives the normalized charge moments $\mathcal{Z}_n(\mathbf{g})$. Therefore, for a critical system, we expect

$$\mathcal{Z}_n(\mathbf{g}) = e^{-T_n(\mathbf{g})\ell + O(1)}\ell^{-\beta_n(\mathbf{g})}, \qquad (2.18)$$

where the coefficient $\beta_n(\mathbf{g})$ is universal and can be computed in the infrared (IR) CFT that describes the critical system. It depends on the specific CFT and the nature of the defects corresponding to the group G under study, and we do not have a generic expression for it. Its computation has to be worked out case by case. In this paper, we calculate it in the massless Majorana fermion field theory for a U(1) group for which the defects are marginal.

2.2.3 Asymptotic behavior

Before delving into the study of the charged moments and entanglement asymmetry in a particular theory, it is insightful to explore the implications of the generic result of eq. (2.18) for the asymptotic behavior of the entanglement asymmetry in the limit of large subsystem size ℓ.

When we plug eq. (2.18) in eq. (2.8), we have to perform an n-fold integral over the group G. Since the leading term in eq. (2.18) decays exponentially with ℓ, the main contribution to this integral comes from the points $\mathbf{h} \in G^n$ where $\mathcal{Z}_n(\mathbf{h}) = 1$ (i.e. where both $T_n(\mathbf{h})$ and $\beta_n(\mathbf{h})$ vanish). These correspond to the elements of G that leave the reduced density matrix ρ_A invariant and form a symmetry subgroup H of G. i.e.

$$H = \left\{ h \in G \mid U_{A,h}\rho_A U_{A,h}^{\dagger} = \rho_A \right\}. \qquad (2.19)$$

Therefore, the strategy is to perform a saddle point approximation of the integral (2.8) around the points $\mathbf{h} \in H^n$; see also refs. [4, 5, 7, 13].

For simplicity, let us assume that H is a finite subgroup. In the integral (2.7) the numerator $\text{tr}(U_{A,g_1} \rho_A U_{A,g_1^{-1}} \ldots U_{A,g_n} \rho_A U_{A,g_n^{-1}})$ is invariant under a right multiplication $(g_1, \ldots, g_n) \mapsto (g_1 h_1, \ldots, g_n h_n)$. Consequently, all the saddle points $\mathbf{h} \in H^n$ contribute equally. Then, to calculate the integral (2.8) for $\ell \gg 1$, we can expand it around the identity point $(\text{Id}, \ldots, \text{Id}) \in G^n$, where Id is the identity in G, and multiply the result by the total number of saddle points, which is given in terms of the cardinality $|H|$ of H as $|H|^{n-1}$. We finally perform the integral by choosing some local coordinates on the group around the identity.

In a neighborhood $\mathcal{U}_{\text{Id}} \subset G$ of the identity, the group elements g can be written as $g = e^{iX}$, where X is an element of the Lie algebra $\mathfrak{g}$ associated with G, of dimension $d = \dim G$. Let $\{J_a\}$, $a = 1, \ldots, d$, be generators of $\mathfrak{g}$, if we take the local coordinate chart $\text{x} = (x_1, \ldots, x_d) \in \mathbb{R}^d \mapsto g(\text{x}) = e^{i \sum_a x_a J_a}$, then, for an arbitrary function $f(g)$ on G, we have

$$\int_{\mathcal{U}_{\text{Id}}} \mathrm{d}g \, f(g) = \int_{g^{-1}(\mathcal{U}_{\text{Id}})} \mu(\text{x}) \, \mathrm{d}\text{x} \, f(g(\text{x})), \tag{2.20}$$

where $\mu(\text{x}) \, \mathrm{d}x$ is the Haar measure of G in the local coordinates x. Since we have to perform an n-fold integral over G, we denote by $\mathbf{x}$ the coordinates for G^n, that is $\mathbf{x} = (\text{x}_1, \ldots, \text{x}_n) \in \mathbb{R}^{dn}$. Now we can express the exponents $T_n(\mathbf{g})$ and $\beta_n(\mathbf{g})$ of the charged moments (2.18) in coordinates and expand them around the identity, which corresponds to $\mathbf{x} = \mathbf{0}$,

$$T_n(\mathbf{g}(\mathbf{x})) = \frac{1}{2} \mathbf{x}^{\text{t}} \mathsf{H}_{T_n} \mathbf{x} + O(\mathbf{x}^3),$$
$$\beta_n(\mathbf{g}(\mathbf{x})) = \frac{1}{2} \mathbf{x}^{\text{t}} \mathsf{H}_{\beta_n} \mathbf{x} + O(\mathbf{x}^3), \tag{2.21}$$

where H_{T_n} and H_{β_n} are $dn \times dn$ Hessian matrices, made of $n \times n$ blocks of dimension $d \times d$. Therefore, in the local coordinate chart that we are considering, for large ℓ the n-fold integral (2.8) reads

$$\int_{G^n} \mathcal{Z}_n(\mathbf{g}) \delta\left(\prod_j g_j \right) \mathrm{d}\mathbf{g} \sim |H|^{n-1} \mu(0)^{n-1} \int_{\mathbb{R}^{dn}} \mathrm{d}\mathbf{x} \, e^{-\frac{1}{2}\mathbf{x}^{\text{t}}(\mathsf{H}_{T_n}\ell + \mathsf{H}_{\beta_n} \log \ell)\mathbf{x}} \delta\left(\sum_{j=1}^{n} \text{x}_j \right). \tag{2.22}$$

Here the factor $|H|^{n-1}$ counts the total number of saddle points. In coordinates, the Dirac delta $\delta\left(\prod_j g_j \right)$ over the group G is replaced by $\delta\left(\sum_{j=1}^{x} \text{x}_j \right) / \mu(0)$. Notice that we have also expanded the measure $\mu(\text{x})$ around $\text{x} = 0$ and restricted to the zeroth order term $\mu(0)$ since the next order terms yield subleading corrections in ℓ.

Since $T_n(\mathbf{g})$ is the sum of the contributions of each defect line according to eq. (2.14), H_{T_n} is block diagonal, $\mathsf{H}_{T_n} = \mathbb{1}_n \otimes \mathsf{H}_t$, where H_t is the $d \times d$ dimensional Hessian of $t(g(x))$. Due to the cyclic property of the trace, the coefficient $\beta_n(\mathbf{g})$ is symmetric under cyclic permutations of the entries g_j of $\mathbf{g}$. Thus H_{β_n} is a block-circulant matrix; that is, it has the block structure

$$\mathsf{H}_{\beta_n} = \begin{pmatrix} \mathsf{C}_1 & \mathsf{C}_n & \cdots & \mathsf{C}_3 & \mathsf{C}_2 \\ \mathsf{C}_2 & \mathsf{C}_1 & \mathsf{C}_n & & \mathsf{C}_3 \\ \vdots & \mathsf{C}_2 & \mathsf{C}_1 & \ddots & \vdots \\ \mathsf{C}_{n-1} & & \ddots & \ddots & \mathsf{C}_n \\ \mathsf{C}_n & \mathsf{C}_{n-1} & \cdots & \mathsf{C}_2 & \mathsf{C}_1 \end{pmatrix}, \tag{2.23}$$

with blocks C_j of size $d \times d$. A block-circulant matrix can be diagonalized in blocks D_p, $p = 0, \ldots, n-1$, with a Fourier transform of the blocks C_j,

$$\mathsf{D}_p = \sum_{j=1}^{n} \mathsf{C}_j e^{i\frac{2\pi}{n}jp}. \tag{2.24}$$

Therefore, if we apply the change of variables

$$\mathrm{x}_j = \frac{1}{\sqrt{n}} \sum_{p=0}^{n-1} \omega_p e^{-i\frac{2\pi}{n}jp}, \qquad j = 1, \ldots, n, \tag{2.25}$$

then the integral (2.22) becomes

$$\int_{G^n} \mathcal{Z}_n(\mathbf{g}) \delta\left(\prod_j g_j\right) \mathrm{d}\mathbf{g} \sim \frac{|H|^{n-1}\mu(0)^{n-1}}{\sqrt{n}} \int_{\mathbb{R}^{dn}} \mathrm{d}\boldsymbol{\omega} e^{-\frac{1}{2}\sum_{p=0}^{n-1} \omega_p(\mathsf{H}_t\ell + \mathsf{D}_p \log \ell)\omega_p} \delta\left(\omega_0\right). \tag{2.26}$$

Integrating out the variable ω_0, we find

$$\int_{G^n} \mathcal{Z}_n(\mathbf{g}) \delta\left(\prod_j g_j\right) \mathrm{d}\mathbf{g} \sim \frac{|H|^{n-1}\mu(0)^{n-1}}{\sqrt{n}} \prod_{p=1}^{n-1} \int_{\mathbb{R}^d} \mathrm{d}\omega\, e^{-\frac{1}{2}\omega(\mathsf{H}_t\ell + \mathsf{D}_p \log \ell)\omega}. \tag{2.27}$$

The remaining integral is Gaussian and we can easily perform it, if we assume that $\mathsf{H}_t\ell + \mathsf{D}_p \log \ell$ is a symmetric definite-positive matrix,

$$\int_{\mathbb{R}^d} \mathrm{d}\omega e^{-\frac{1}{2}\omega(\mathsf{H}_t\ell + \mathsf{D}_p \log \ell)\omega} = \left(\det\left(2\pi(\mathsf{H}_t\ell + \mathsf{D}_p \log \ell)^{-1}\right)\right)^{1/2}. \tag{2.28}$$

Plugging it in eq. (2.27), we obtain

$$\int_{G^n} \mathcal{Z}_n(\mathbf{g}) \delta\left(\prod_j g_j\right) \mathrm{d}\mathbf{g} \sim \frac{(2\pi\ell)^{\frac{d(1-n)}{2}}}{\sqrt{n}} \left(\frac{|H|\mu(0)}{\sqrt{\det \mathsf{H}_t}}\right)^{n-1} \prod_{p=0}^{n-1} \left(\det\left(\mathbb{1} + \mathsf{H}_t^{-1}\mathsf{D}_p \frac{\log \ell}{\ell}\right)\right)^{1/2}. \tag{2.29}$$

This result is independent of the local coordinate chart that we consider to perform the integration. In fact, under a change of local coordinates $\mathrm{x} \mapsto \mathrm{y}(\mathrm{x})$, the measure $\mu(\mathrm{x})$ transforms as $\mu(\mathrm{x}) = \left|\det(\partial y^\sigma/\partial x^b)\right| \mu'(\mathrm{y})$ and, because quadratic forms are $(0,2)$-tensor fields, the determinant of the Hessian H_t transforms as $\det \mathsf{H}_t(\mathrm{x}) = \left|\det(\partial y^\sigma/\partial x^b)\right|^2 \det \mathsf{H}_t'(\mathrm{y})$. Therefore, the quotient $\mu(0)/\sqrt{\det \mathsf{H}_t}$ is coordinate independent. The same applies for the terms $\det(\mathbb{1} + \mathsf{H}_t^{-1}\mathsf{D}_p \log \ell/\ell)$.

Finally, applying (2.29) in eq. (2.8) and using the identity $\log\det M = \operatorname{tr}\log M$ for a matrix M, we find that the Rényi entanglement asymmetry for a compact Lie group G in the ground state of a critical one dimensional quantum system behaves as

$$\Delta S_A^{(n)} = \frac{\dim G}{2} \log \ell + a_n + b_n \frac{\log \ell}{\ell} + \cdots, \tag{2.30}$$

where

$$a_n = \log \frac{\operatorname{vol} G}{|H|} + \frac{1}{2} \log \frac{n^{\frac{1}{n-1}} \det \mathsf{H}_t}{(2\pi)^{\dim G}\mu(0)^2}, \tag{2.31}$$

and

$$b_n = \frac{1}{2(n-1)} \sum_{p=1}^{n-1} \text{tr}\left(\mathsf{D}_p \mathsf{H}_t^{-1}\right).$$ (2.32)

Eq. (2.30) is the first main result of this paper. We stress that the first two terms in (2.30), of order $O(\log \ell)$ and $O(1)$ respectively, have already been observed in the XY spin chain when considering the particle number U(1) (a)symmetry [4], and more generically for matrix product states in ref. [13]. Crucially, what is new here is the last term in eq. (2.30), of order $O(\log \ell/\ell)$. While the terms of order $O(\log \ell)$ and $O(1)$ are present in the ground state of critical and non-critical systems alike, the term of order $O(\log \ell/\ell)$ only appears when the system is at a critical point.

This $\log \ell/\ell$ term appears only when the exponent $\beta_n(\mathbf{g})$ in eq. (2.18) is non-zero. Although this exponent is universal, the coefficient b_n is non-universal since it also depends on the defect tension $T_n(\mathbf{g})$ (via H_t), which is cut-off dependent. Semi-universal corrections of the form $\log \ell/\ell$ have been found in, e.g., the corner free energy in critical systems [74] and in the ground state full counting statistics of the critical XY spin chain [75].

We finally discuss the group structures that were not considered earlier. When both G and H are finite, it is straightforward to show that the logarithmic term is vanishing, the $O(1)$ term is just $\log(|G|/|H|)$ and there are no $\log \ell/\ell$ corrections (see also [13]). When both G and H are continuous, the leading $\log \ell$ term has a prefactor equal to $(\dim G - \dim H)/2$, but the explicit expressions for the subleading terms are more cumbersome and not very illuminating.

3 The XY spin chain and the massless Majorana fermion field theory

In the rest of the paper, we focus on a particular gapless system: the XY spin chain at the Ising critical line. We consider its ground state, and compute the charged moments and the Rényi entanglement asymmetry associated with the rotations of the spin around the z-axis.

The Hamiltonian of the XY spin chain is

$$H_{\text{XY}} = -\frac{1}{2} \sum_{j \in \mathbb{Z}} \left(\frac{1+\gamma}{2} \sigma_j^x \sigma_{j+1}^x + \frac{1-\gamma}{2} \sigma_j^y \sigma_{j+1}^y + h \sigma_j^z\right),$$ (3.1)

where σ_j^α are the Pauli matrices at the site j. The parameter γ tunes the anisotropy between the couplings in the x and y components of the spin and h is the strength of the transverse magnetic field. The XY spin chain is gapless along the lines $\gamma = 0$, $|h| < 1$ and $\gamma \neq 0$, $|h| = 1$ in parameter space, and the scaling limits along those lines are respectively the massless Dirac and Majorana fermion field theories.

For $\gamma \neq 0$, the Hamiltonian of eq. (3.1) is not invariant under the rotations $U_\alpha = e^{i\alpha Q}$ around the z-axis, generated by the transverse magnetization

$$Q = \frac{1}{2} \sum_{j \in \mathbb{Z}} (\sigma_j^z - \mathbb{I}),$$ (3.2)

except for $\alpha = \pi$, which corresponds to the $\mathbb{Z}_2$ spin flip symmetry. The entanglement asymmetry associated with this U(1) symmetry has been thoroughly studied in ref. [4] for the ground state of (3.1) outside the critical lines $\gamma \neq 0$, $|h| = 1$ using exact methods on the

lattice. In that case, the charged moments $\mathcal{Z}_n(\boldsymbol{\alpha})$ decay exponentially for large subsystem size ℓ as in eq. (2.15), where the coefficient $T_n(\boldsymbol{\alpha}) = \sum_{j=1}^{n} t(\alpha_j)$ is the sum of the string tension $t(\alpha_j)$ of each defect, which here is given by [4]

$$t(\alpha) = - \int_{-\pi}^{\pi} \frac{\mathrm{d}k}{4\pi} \log(i \cos \xi_k \sin \alpha + \cos \alpha), \tag{3.3}$$

with

$$e^{i\xi_k} = \frac{h - \cos k + i\gamma \sin k}{\sqrt{(h - \cos k)^2 + \gamma^2 \sin^2 k}}. \tag{3.4}$$

Note that the string tension $t(\alpha)$ is not real; as we will see in section 4, this is related to the fact that the gluing conditions of the defects associated with this U(1) group make the theory non-Hermitian.

To obtain the Rényi entanglement asymmetry, we can apply the general result of eq. (2.30). In this case, since $G = \mathrm{U}(1)$, we have that $\dim G = 1$, $\mathrm{vol}\, G = 2\pi$, $\mu(0) = 1$, and the symmetric subgroup is the $\mathbb{Z}_2$ spin-flip symmetry, $H = \mathbb{Z}_2$. Since $\dim G = 1$, the block H_t is a scalar and it is given by eq. (3.3) such that $\mathsf{H}_t = t''(0) = \partial^2 t(\alpha)/\partial \alpha^2|_{\alpha=0}$.

In ref. [4], the following result was derived for the XY chain out of the critical line $|h| = 1$:

$$\Delta S_A^{(n)} = \frac{1}{2} \log \ell + \frac{1}{2} \log \frac{\pi t''(0) n^{1/(n-1)}}{2} + O(\ell^{-1}), \tag{3.5}$$

with

$$t''(0) = \begin{cases} \frac{1}{2} \frac{\gamma}{\gamma+1}, & |h| < 1, \\ \frac{1}{2} \frac{\gamma^2}{1-\gamma^2} \left(\frac{|h|}{\sqrt{h^2+\gamma^2-1}} - 1 \right), & |h| > 1. \end{cases} \tag{3.6}$$

Notice that $t''(0)$ is continuous at $|h| = 1$, reflecting the fact that this result also applies along the critical line. Indeed, in this case, the string tension $T_n(\boldsymbol{\alpha})$ is still given by eq. (3.3), and following the same steps as in ref. [4] one arrives at the same result.

However, crucially for this paper, along the critical line $\gamma \neq 0$, $|h| = 1$, we also expect that the charged moments $\mathcal{Z}_n(\boldsymbol{\alpha})$ contain the algebraically decaying factor of eq. (2.18), according to the general reasoning of section 2.2.3. However, an analytical expression for the coefficient $\beta_n(\boldsymbol{\alpha})$ is unknown. In what follows, we will obtain it by exploiting the conformal invariance of the underlying field theory.

As we have already mentioned, the scaling limit of the XY spin chain (3.1) along the critical lines $\gamma \neq 0$, $|h| = 1$ is the massless Majorana fermion field theory, whose Hamiltonian is

$$H = \frac{1}{2i} \int_{\mathbb{R}} \psi(x) \partial_x \psi(x) - \bar{\psi}(x) \partial_x \bar{\psi}(x) \, \mathrm{d}x, \tag{3.7}$$

where the Majorana fields $\psi(x)$ and $\bar{\psi}(x)$ satisfy the algebra

$$\{\psi(x), \psi(y)\} = \delta(x - y), \qquad\qquad \psi^\dagger(x) = \psi(x), \tag{3.8}$$

$$\{\bar{\psi}(x), \bar{\psi}(y)\} = \delta(x - y), \qquad\qquad \bar{\psi}^\dagger(x) = \bar{\psi}(x), \tag{3.9}$$

and $\{\psi(x), \bar{\psi}(y)\} = 0$. The U(1) charge operator in eq. (3.2) corresponds in this field theory to

$$Q = i \int_{\mathbb{R}} \psi(x) \bar{\psi}(x) \, \mathrm{d}x. \tag{3.10}$$

The details on the derivation of the Hamiltonian (3.1) and Q in the continuum limit are reported in appendix A.

The transformations

$$U_{A,\alpha} = e^{i\alpha Q_A} = \exp\left(-\alpha \int_A \psi(x)\bar{\psi}(x)\,\mathrm{d}x\right) \tag{3.11}$$

generated by the charge (3.10) in a subsystem A act on the fields $\psi(x)$, $\bar{\psi}(x)$ in the following way

$$U_{A,\alpha}^{\dagger}\Psi(x)U_{A,\alpha} = \tilde{R}_\alpha \Psi(x), \qquad \text{if } x \in A, \tag{3.12}$$
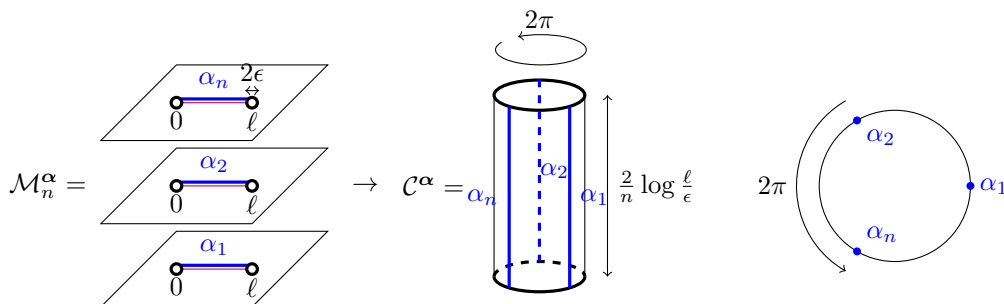
with

$$\Psi = \begin{pmatrix} \psi \\ \bar{\psi} \end{pmatrix}, \quad \tilde{R}_\alpha = \begin{pmatrix} \cos\alpha & -\sin\alpha \\ \sin\alpha & \cos\alpha \end{pmatrix} \in \mathrm{SO}(2). \tag{3.13}$$

The group action consists of a rotation that mixes ψ and $\bar{\psi}$. In general, this is not a symmetry of the theory, unless $\alpha = \pi$, for which $\psi \mapsto -\psi$ and $\bar{\psi} \mapsto -\bar{\psi}$. For α purely imaginary, the defect can be realized in the classical 2d Ising model by rescaling the couplings on all the bonds that intersect the defect line. A dictionary between the two realizations is given, e.g., in [36].

Crucially for our analysis, the field $\psi(x)\bar{\psi}(x)$ has scaling dimension 1, therefore the line defect implemented by $U_{A,\alpha}$ corresponds to a marginal perturbation of the CFT action along the line. This is very important for the calculations reported in section 4, as it introduces a non-trivial dependence of the CFT partition function on the defect strength α. Indeed, if the perturbation were instead irrelevant, then the effects of the defect would be renormalized to zero in the IR limit. If the perturbation were relevant, then the defect would flow to some fixed point in the IR, corresponding to some boundary condition along the line, and the CFT partition function would also be independent on the precise value of α. For instance, such a situation would occur if we looked at the asymmetry with respect to rotations around the x-axis, as opposed to the z-axis, corresponding to replacing σ_j^z with σ_j^x in eq. (3.2). In the CFT, this would then correspond to a perturbation by the relevant operator $\sigma(x)$ with scaling dimension $1/8$. The defect line would flow to a fixed boundary condition in the IR, and this would completely change the way we do the analysis, see in particular ref. [76] for more details on that situation.

4 Calculation of the scaling dimension associated to n defects in the Majorana CFT

In section 2.2, we have seen that the charged moments $\mathcal{Z}_n(\boldsymbol{\alpha})$ can be cast as the ratio $Z(\mathcal{M}_n^{\boldsymbol{\alpha}})/Z(\mathcal{M}_n)$ between the partition function $Z(\mathcal{M}_n^{\boldsymbol{\alpha}})$ of the model on the n-sheet Riemann surface $\mathcal{M}_n$ with n defect lines with strengths $\boldsymbol{\alpha} = (\alpha_1, \ldots, \alpha_n)$ along its branch cuts and the one, $\mathcal{Z}(\mathcal{M}_n)$, without them. As we discussed, in critical systems, this ratio contains a universal term $Z_{\mathrm{CFT}}(\mathcal{M}_n^{\boldsymbol{\alpha}})/Z_{\mathrm{CFT}}(\mathcal{M}_n)$, fully determined by the CFT that describes the low-energy physics. In this section, we study it in the massless Majorana fermion theory (3.7) for the marginal defect lines (3.11).

Figure 4. On the left, we represent the n-sheet Riemann surface $\mathcal{M}_n$ with n marginal defect lines inserted along the branch cut $[0, \ell]$ of each replica sheet, which arises in the calculation of the ground state charged moments $\mathcal{Z}_n(\boldsymbol{\alpha})$. At the branch points 0 and ℓ, two disks of radius ϵ have been removed as UV cut-off. Under the conformal transformation (4.4), $\mathcal{M}_n$ is mapped into the cylinder $\mathcal{C}$ on the middle, of circumference 2π and height $\frac{2}{n} \log \frac{\ell}{\epsilon}$. The defect lines in $\mathcal{M}_n$ are mapped into n evenly spaced vertical defects at the points $x_j = \frac{2\pi j}{n}, j = 1, \ldots, n$. The CFT partition functions on these two surfaces with the marginal defects are equal. On the right, top view of the cylinder $\mathcal{C}$ with the defects.

When there are no defects, it is well-known [10–12] that, for a generic CFT,

$$\frac{Z_{\text{CFT}}(\mathcal{M}_n)}{Z_{\text{CFT}}(\mathcal{M})^n} \propto \ell^{-2\delta_n}, \qquad \delta_n = \frac{c}{12}\left(n - \frac{1}{n}\right), \tag{4.1}$$

where c is the central charge of the CFT, which for the massless Majorana fermion is $c = 1/2$.

In the massless Majorana fermion theory, when we insert the n marginal defect lines along each branch cut of the surface $\mathcal{M}_n$, the result (4.1) changes as

$$\frac{Z_{\text{CFT}}(\mathcal{M}_n^{\boldsymbol{\alpha}})}{Z_{\text{CFT}}(\mathcal{M})^n} \propto \ell^{-2\left(\delta_n + \frac{\tilde{\Delta}_n(\boldsymbol{\alpha})}{n}\right)}, \tag{4.2}$$

as we will show below. The contribution of the n marginal defects is encoded in the exponent $\tilde{\Delta}_n(\boldsymbol{\alpha})$. Then the ratio of the partition functions on the surface $\mathcal{M}_n$ with and without defects is

$$\frac{Z_{\text{CFT}}(\mathcal{M}_n^{\boldsymbol{\alpha}})}{Z_{\text{CFT}}(\mathcal{M}_n)} = \ell^{-\frac{2}{n}\tilde{\Delta}_n(\boldsymbol{\alpha})}, \tag{4.3}$$

and, comparing with eq. (2.18), $\beta_n(\boldsymbol{\alpha}) = \frac{2}{n}\tilde{\Delta}_n(\boldsymbol{\alpha})$. The rest of the section will be devoted to deriving eq. (4.2) and computing explicitly the coefficient $\tilde{\Delta}_n(\boldsymbol{\alpha})$.

4.1 Conformal mapping to the cylinder with n defect lines

To determine the partition function $Z_{\text{CFT}}(\mathcal{M}_n^{\boldsymbol{\alpha}})$ with the n marginal defect lines, we perform the conformal transformation

$$z \mapsto w(z) = i \log\left[\left(\frac{z}{z - \ell}\right)^{1/n}\right]. \tag{4.4}$$

If at the branch points $z = 0$ and $z = \ell$ of the Riemann surface $\mathcal{M}_n$ we remove a disk of radius ϵ as a UV cut-off, then eq. (4.4) maps $\mathcal{M}_n$ to a cylinder with circumference 2π and height $W = \frac{2}{n} \log(\ell/\epsilon)$, which we denote as $\mathcal{C}$, see figure 4. We choose as coordinates of the cylinder $w = x + i\tau$, with $x \sim x + 2\pi$ and $\tau \in [-\frac{1}{n} \log(\ell/\epsilon), \frac{1}{n} \log(\ell/\epsilon)]$.

Under eq. (4.4), the n branch cuts $[0, \ell]$ of $\mathcal{M}_n$ are mapped to the equally-spaced lines $x_j = \frac{2\pi j}{n}$, $j = 1, \ldots, n$ ($x_n = 2\pi$ is identified with $x = 0$) on the cylinder, as we illustrate in figure 4. Thus, on the cylinder $\mathcal{C}$, the n marginal defects are inserted along these lines. We assume the Majorana fields $\psi, \bar{\psi}$ to have trivial monodromy on $\mathcal{M}_n$ along the cycle that connects all the replicas. Therefore, after the map (4.4), these fields satisfy anti-periodic boundary conditions on the cylinder since they have half-integer spin [77].

The next step is to carefully determine the gluing condition that is satisfied by the Majorana fields ψ and $\bar{\psi}$ across each defect after the conformal map (4.4) to the cylinder. In the previous section, we found that, on the Riemann surface $\mathcal{M}_n$, the gluing condition across a defect with strength α_j is given by eq. (3.12), i.e.

$$\Psi(z = x + i0^+) = \tilde{R}_{\alpha_j} \Psi(z = x + i0^-), \qquad \text{for} \quad x \in [0, \ell], \tag{4.5}$$

where the 2×2 matrix $\tilde{R}_{\alpha_j}$ is defined in eq. (3.13). Crucially, this gluing condition changes under the conformal transformation (4.4). Indeed, since the Majorana fields ψ and $\bar{\psi}$ are primaries with conformal dimension $1/2$, they transform as

$$\psi(w) = \left(\frac{dw}{dz}\right)^{-1/2} \psi(z), \qquad \bar{\psi}(\bar{w}) = \left(\frac{d\bar{w}}{d\bar{z}}\right)^{-1/2} \bar{\psi}(\bar{z}). \tag{4.6}$$

Combining this with eq. (4.5) and noting that a point slightly above the defect on $\mathcal{M}_n$ (i.e. at $z = x + i0^+$) is mapped to a point slightly to the left of the defect on the cylinder (i.e. at $w = x_j + i\tau + 0^-$), we find that the condition that ψ and $\bar{\psi}$ must satisfy across the defect at the line $x_j = \frac{2\pi j}{n}$ on the cylinder $\mathcal{C}$ is

$$\Psi(w = x_j + i\tau + 0^-) = R_{i\alpha_j} \Psi(w = x_j + i\tau + 0^+), \tag{4.7}$$

where we define

$$R_{i\alpha_j} = \begin{pmatrix} \left(\frac{dw}{dz}\right)^{-1/2} & 0 \\ 0 & \left(\frac{d\bar{w}}{d\bar{z}}\right)^{-1/2} \end{pmatrix} \tilde{R}_{\alpha_j} \begin{pmatrix} \left(\frac{dw}{dz}\right)^{1/2} & 0 \\ 0 & \left(\frac{d\bar{w}}{d\bar{z}}\right)^{1/2} \end{pmatrix} = \begin{pmatrix} \cos \alpha_j & i \sin \alpha_j \\ i \sin \alpha_j & \cos \alpha_j \end{pmatrix}. \tag{4.8}$$

Observe that, in the first equality, we can take out a factor $\left|\frac{dw}{dz}\right|^{-1/2}$ from the first matrix and a factor $\left|\frac{dw}{dz}\right|^{1/2}$ from the third one. Taking into account that $\frac{dw}{dz} / \left|\frac{dw}{dz}\right| = i$ for $z = x + i0^+$, we find the second equality.

In summary, using the conformal transformation (4.4), the partition function $Z_{\text{CFT}}(\mathcal{M}_n^{\alpha})$ of the massless Majorana fermion with n marginal defect lines at the branch cuts of the surface $\mathcal{M}_n$ is equal to the partition function $Z_{\text{CFT}}(\mathcal{C}^{\alpha})$ of the theory on the cylinder $\mathcal{C}$ with n equally-spaced defect lines along its longitudinal direction and described by the gluing conditions (4.7). If we impose conformal boundary conditions $|a\rangle$ and $|b\rangle$ at the extremes of the cylinder $\mathcal{C}$, the partition function $Z_{\text{CFT}}(\mathcal{C}^{\alpha})$ can be written as

$$Z_{\text{CFT}}(\mathcal{C}^{\alpha}) = \langle a| e^{-WH} |b\rangle, \tag{4.9}$$

where H is the Hamiltonian of the free Majorana fermion (3.7) defined on a circle of length 2π with the fields ψ and $\bar{\psi}$ satisfying the gluing conditions (4.8) at the points

$x_j = \frac{2\pi j}{n}$, $j = 1, \ldots, n$ with strengths $\alpha = \alpha_1, \alpha_2, \ldots, \alpha_n$ respectively. Alternatively, as we show in detail in appendix B, these conditions can be explicitly implemented in the Hamiltonian (3.7) by including in it n point defects of the form $\psi(x_j)\bar{\psi}(x_j)$,

$$H = \frac{1}{2i} \int_0^{2\pi} (\psi\partial_x\psi - \bar{\psi}\partial_x\bar{\psi})\,\mathrm{d}x + \sum_{j=1}^n i\mu_j\psi(x_j)\bar{\psi}(x_j), \tag{4.10}$$

where the parameters μ_j are related to the strength of the defects by $\mu_j/2 = i\arctan(\alpha_j/2)$.

For $W \gg 2\pi$, i.e. for large subsystem length ℓ, the dominant term in the partition function (4.9) is given by the ground state energy $E(\boldsymbol{\alpha})$ of the Hamiltonian with defects (4.10),

$$Z_{\mathrm{CFT}}(\mathcal{C}^{\boldsymbol{\alpha}}) \propto e^{-WE(\boldsymbol{\alpha})}. \tag{4.11}$$

The ground state energy should satisfy the usual CFT formula

$$E(\boldsymbol{\alpha}) = \tilde{\Delta}_n(\boldsymbol{\alpha}) - \frac{c}{12}, \tag{4.12}$$

where $\tilde{\Delta}_n(\boldsymbol{\alpha})$ takes into account the contribution of the defects and, consequently, it vanishes, $\tilde{\Delta}_n(\mathbf{0}) = 0$, in their absence. It may be interpreted as the scaling dimension of a n-defect insertion operator. Combining the two previous equations, and taking into account that $W = \frac{2}{n}\log(\ell/\epsilon)$, we arrive at eq. (4.2). Therefore, since $\tilde{\Delta}_n(\boldsymbol{\alpha}) = E(\boldsymbol{\alpha}) - E(\mathbf{0})$, the problem of computing the scaling dimension $\tilde{\Delta}_n(\boldsymbol{\alpha})$ boils down to determining the ground state energy of the Hamiltonian (4.10) with n point defects. We will devote the rest of this section to calculating it.

However, before proceeding, it is important to note that the gluing condition (4.8) on the cylinder presents an issue: if $\alpha \in \mathbb{R}$, it does not respect the self-adjointness of the Majorana fields $\psi(w)$ and $\bar{\psi}(\bar{w})$. The same problem arises in the Hamiltonian with defects (4.10), which is not Hermitian for $\alpha \in \mathbb{R}$. To calculate $\tilde{\Delta}_n(\boldsymbol{\alpha})$, it is important that the Hamiltonian is Hermitian to ensure that its spectrum is real and, therefore, the energy of its ground state is well-defined. In order to cure this problem, we can analytically continue the defect strength $\alpha \to -i\lambda$ with $\lambda \in \mathbb{R}$. This changes the 2×2 gluing matrix (4.8)

$$R_{i\alpha} \to R_\lambda = \begin{pmatrix} \cosh\lambda & \sinh\lambda \\ \sinh\lambda & \cosh\lambda \end{pmatrix}. \tag{4.13}$$

Since all its entries are real, it is now compatible with the self-adjointness of the Majorana fields. This analytic continuation also makes the Hamiltonian with defects (4.10) Hermitian. In the following, we carry out the calculation of the ground state energy assuming that the gluing matrix is (4.13) with $\lambda \in \mathbb{R}$. We will eventually take $\lambda \to i\alpha$ in the final result, which we check against exact numerical calculations in the XY spin chain.

4.2 Ground state energy for a single defect ($n = 1$)

We start by solving the case of a single marginal defect. We take the spatial coordinate x defined on the interval $x \in [-\pi, \pi]$ with the points $x = -\pi$ and π identified and, for simplicity, we put the defect at $x = 0$. We impose the following boundary conditions for the fields $\psi(x)$, $\bar{\psi}(x)$ at $x = 0$ and $x = \pi$:

$$\Psi(0^-) = R_\lambda\Psi(0^+), \qquad\qquad \Psi(-\pi) = -\Psi(\pi). \tag{4.14}$$

The first one is the gluing condition for the defect, while the second one is the anti-periodic boundary condition. With these boundary conditions imposed on the fields, the Hamiltonian is

$$H = \frac{1}{2i} \int_{-\pi}^{0} dx\, \Psi^\dagger D \Psi \,+\, \frac{1}{2i} \int_{0}^{\pi} dx\, \Psi^\dagger D \Psi, \qquad D = \begin{pmatrix} \partial_x & 0 \\ 0 & -\partial_x \end{pmatrix}. \tag{4.15}$$

4.2.1 Diagonalization of the Hamiltonian

The goal now is to diagonalize the Hamiltonian (4.15). To do this, we look for pairs of functions $(u(x), v(x))$ that satisfy the same gluing and anti-periodic boundary conditions as $\Psi(x)$,

$$\begin{pmatrix} u(0^-) \\ v(0^-) \end{pmatrix} = R_\lambda \begin{pmatrix} u(0^+) \\ v(0^+) \end{pmatrix}, \quad \begin{pmatrix} u(-\pi) \\ v(-\pi) \end{pmatrix} = - \begin{pmatrix} u(\pi) \\ v(\pi) \end{pmatrix}, \tag{4.16}$$

and are eigenstates of the differential operator $\frac{1}{i}D$. These are piecewise plane waves,

$$u_k(x) = \begin{cases} A_0 e^{ikx}, & x \in (-\pi, 0), \\ A_1 e^{ikx}, & x \in (0, \pi), \end{cases} \qquad v_k(x) = \begin{cases} B_0 e^{-ikx}, & x \in (-\pi, 0), \\ B_1 e^{-ikx}, & x \in (0, \pi). \end{cases} \tag{4.17}$$

If they satisfy the boundary conditions, then such wavefunctions are automatically eigenfunctions of $\frac{1}{i}D$ with eigenvalue k.

The conditions (4.16) impose the following constraints on the amplitudes:

$$\begin{pmatrix} A_0 \\ B_0 \end{pmatrix} = R_\lambda \begin{pmatrix} A_1 \\ B_1 \end{pmatrix}, \qquad \begin{pmatrix} A_0 e^{-ik\pi} \\ B_0 e^{ik\pi} \end{pmatrix} = - \begin{pmatrix} A_1 e^{ik\pi} \\ B_1 e^{-ik\pi} \end{pmatrix}. \tag{4.18}$$

This linear system of equations admits a non-zero solution if and only if

$$\det \left[\mathbb{I} + R_\lambda \begin{pmatrix} e^{-ik2\pi} & 0 \\ 0 & e^{ik2\pi} \end{pmatrix} \right] = 0. \tag{4.19}$$

Let us introduce the polynomial

$$P_\lambda(z) = z \det \left[\mathbb{I} + R_\lambda \begin{pmatrix} 1/z & 0 \\ 0 & z \end{pmatrix} \right] \tag{4.20}$$

of degree 2. Eq. (4.19) is equivalent to the polynomial equation

$$P_\lambda(z) = 0 \tag{4.21}$$

for the variable $z = e^{i2\pi k}$. From the explicit form of R_λ, we find that $P_\lambda(z)$ is

$$P_\lambda(z) = \text{const.} \times (z - e^{i\theta})(z - e^{-i\theta}), \tag{4.22}$$

with

$$\theta = 2 \arctan\left(\tanh \frac{\lambda}{2}\right) + \pi \ \in [0, 2\pi). \tag{4.23}$$

Then the full set of solutions k of eq. (4.19) is

$$k \in \mathcal{S}_\lambda = \left(\mathbb{Z} + \frac{\theta}{2\pi}\right) \cup \left(\mathbb{Z} - \frac{\theta}{2\pi}\right). \tag{4.24}$$

For each solution $k \in \mathcal{S}_\lambda$, the pair (u_k, v_k) can be used to construct a Bogoliubov mode for the Hamiltonian (4.15), taking the scalar product with the two-component field $(\psi, \bar{\psi})$

$$\eta_k = \int_{-\pi}^{\pi} dx \left[u_k^*(x) \psi(x) + v_k^*(x) \bar{\psi}(x) \right], \tag{4.25}$$

which automatically satisfies $[H, \eta_k] = k \, \eta_k$. Then, using the orthonormality of the set of functions $(u_k(x), v_k(x))$ we get

$$H = \frac{1}{2} \sum_{k \in \mathcal{S}_\lambda} k \eta_k^\dagger \eta_k, \tag{4.26}$$

where the sum in k runs over all the solutions in eq. (4.24) and the modes satisfy the anticommutation relations $\{\eta_k^\dagger, \eta_q\} = \delta_{k,q}$.

Notice that, taking the complex conjugate of the eigenvalue equation for $\frac{1}{i}D$, we get that (u_k^*, v_k^*) is an eigenvector with eigenvalue $-k$,

$$D \begin{pmatrix} u_k \\ v_k \end{pmatrix} = ik \begin{pmatrix} u_k \\ v_k \end{pmatrix} \implies D \begin{pmatrix} u_k^* \\ v_k^* \end{pmatrix} = -ik \begin{pmatrix} u_k^* \\ v_k^* \end{pmatrix}. \tag{4.27}$$

Thus we can set $u_{-k}(x) = u_k^*(x)$ and $v_{-k}(x) = v_k^*(x)$. This implies that $\eta_{-k} = \eta_k^\dagger$, and eq. (4.26) can be rewritten in the form

$$H = \frac{1}{2} \sum_{k \in \mathcal{S}_\lambda} k \, \eta_k \eta_{-k}. \tag{4.28}$$

Alternatively, we can express it as a sum restricted to the set of positive solutions k, $\mathcal{S}_\lambda^+ = \{k \in \mathcal{S}_\lambda \mid k > 0\}$,

$$H = \sum_{k \in \mathcal{S}_\lambda^+} k \, (\eta_k \eta_{-k} - 1/2). \tag{4.29}$$

4.2.2 Ground state energy

From eq. (4.29), it is clear that the ground state of the single-defect Hamiltonian (4.15) is the state annihilated by all the modes η_{-k} for $k \in \mathcal{S}_\lambda^+$. The ground state energy is

$$E(\lambda) = -\frac{1}{2} \sum_{k \in \mathcal{S}^+} k = -\frac{1}{2} \left[\sum_{m=0}^{\infty} \left(m + \frac{\theta}{2\pi} \right) + \sum_{m=1}^{\infty} \left(m - \frac{\theta}{2\pi} \right) \right]. \tag{4.30}$$

These infinite sums can be evaluated by zeta-regularization. Taking into account that

$$\lim_{s \to -1} \sum_{m=0}^{\infty} (m + a)^{-s} = \zeta(-1, a), \tag{4.31}$$

where $\zeta(s, a) = \sum_{m=0}^{\infty} (m + a)^{-s}$ is the Hurwitz zeta function, the ground state energy can be written as

$$E(\lambda) = -\frac{1}{2} \left[\zeta \left(-1, \frac{\theta}{2\pi} \right) + \zeta \left(-1, 1 - \frac{\theta}{2\pi} \right) \right]. \tag{4.32}$$

Using the identity $\zeta(-1, a) = -\frac{1}{12} + \frac{a}{2} - \frac{a^2}{2} = \zeta(-1, 1 - a)$, we arrive at

$$E(\lambda) = \frac{1}{2}\left(\frac{1}{\pi}\arctan\left(\tanh\frac{\lambda}{2}\right)\right)^2 - \frac{1}{24}. \tag{4.33}$$

Identifying this expression with the standard formula for the ground state energy in a CFT,

$$E(\lambda) = \Delta_1(\lambda) - \frac{c}{12}, \tag{4.34}$$

with $c = 1/2$ for the massless Majorana fermion, we find that the scaling dimension associated with the insertion of a single marginal defect of strength λ is

$$\Delta_1(\lambda) = \frac{1}{2\pi^2}\arctan^2\left(\tanh\frac{\lambda}{2}\right). \tag{4.35}$$

4.2.3 Connection with previous works

The scaling dimension associated with a single defect was computed in ref. [19] applying lattice methods in the quantum Ising chain and in ref. [23] using a boundary CFT approach. In the latter, the Ising CFT with a defect is folded along the defect, obtaining a $\mathbb{Z}_2$ orbifold of the compact boson in which the defect is encoded in the boundary condition. The relation between such bosonic boundary condition and our gluing parameter λ can be found in ref. [36].

In the case $n = 1$, the charged moments (2.9) specialize to $\mathcal{Z}_1(\alpha) = \text{Tr}(\rho_A e^{i\alpha Q_A})$. This is the full counting statistics, i.e. the cumulant generating function, of the charge Q_A in the subsystem A. In our setup, it corresponds to the expectation value of a single defect line on the single replica surface $\mathcal{M}$. In the ground state of the critical XY spin chain, this quantity was calculated in refs. [78, 79] employing lattice methods, see also [75, 80, 81], and obtaining that $\mathcal{Z}_1(\alpha) = e^{-t(\alpha)\ell}\ell^{-2\tilde{\Delta}_1(\alpha)}$, with $t(\alpha)$ given by eq. (3.3), and the exponent $\tilde{\Delta}_1(\alpha) = \Delta_1(-i\alpha)$ that we have found in eq. (4.35) using CFT.

Notice that the case $\lambda = i\pi$ corresponds to the $\mathbb{Z}_2$ spin-flip symmetry of the spin chain and the associated defect is topological — the ε Verlinde line [16, 24, 82]. When this line is open, as in our case, two disorder operators $\mu(z)$ are inserted at its end-points [16]. Therefore, by the Kramers-Wannier duality, $\mathcal{Z}_1(\pi)$ should be proportional to the two-point function of the spin fields $\sigma(z)$ at its end-points, $\mathcal{Z}_1(\pi) \propto \langle\sigma(0)\sigma(\ell)\rangle = \ell^{-2\Delta_\sigma}$, which have scaling dimension $\Delta_\sigma = 1/8$, that is precisely $\Delta_1(i\pi)$.

4.3 Ground state energy for n equally-spaced defects

We now extend the calculation of the previous section to the case of multiple defects. In this section we take the spatial coordinate x in the interval $[0, 2\pi]$, and we put the defects at positions $x_j = \frac{2\pi j}{n}$ with $j = 1, \ldots, n$. We also define $x_0 = 0$. The Hamiltonian is

$$H = \sum_{j=1}^{n}\frac{1}{2i}\int_{x_{j-1}}^{x_j}\mathrm{d}x\,\Psi^\dagger D\Psi, \qquad D = \begin{pmatrix} \partial_x & 0 \\ 0 & -\partial_x \end{pmatrix}, \tag{4.36}$$

with the following gluing conditions corresponding to n equally-spaced defects of strengths $\lambda_1, \lambda_2, \ldots, \lambda_n$,

$$\Psi(x_j + 0^-) = R_{\lambda_j}\Psi(x_j + 0^+), \tag{4.37}$$

where the matrix R_λ was defined in eq. (4.13), and the anti-periodic boundary condition $\Psi(0) = -\Psi(2\pi)$.

4.3.1 Diagonalization of the Hamiltonian

To diagonalize that Hamiltonian, we proceed as in the $n = 1$ case. We look for pairs of functions $(u_k(x), v_k(x))$ that satisfy the same gluing conditions as $\Psi(x)$ and are eigenstates of $\frac{1}{i}D$. We look for solutions in the form of piecewise plane waves,

$$
u_k(x) = \begin{cases} A_0 e^{ikx}, & x \in (0, x_1), \\ A_1 e^{ikx}, & x \in (x_1, x_2), \\ \vdots \\ A_n e^{ikx}, & x \in (x_{n-1}, x_n), \end{cases} \qquad v_k(x) = \begin{cases} B_0 e^{-ikx}, & x \in (0, x_1), \\ B_1 e^{-ikx}, & x \in (x_1, x_2), \\ \vdots \\ B_n e^{-ikx}, & x \in (x_{n-1}, x_n). \end{cases} \tag{4.38}
$$

The gluing conditions (4.37) imply the following relations between consecutive amplitudes

$$
\begin{pmatrix} A_{j-1} \\ B_{j-1} \end{pmatrix} = \begin{pmatrix} e^{-ikx_j} & 0 \\ 0 & e^{ikx_j} \end{pmatrix} R_{\lambda_j} \begin{pmatrix} e^{ikx_j} & 0 \\ 0 & e^{-ikx_j} \end{pmatrix} \begin{pmatrix} A_j \\ B_j \end{pmatrix}, \tag{4.39}
$$

while the anti-periodicity condition implies

$$
\begin{pmatrix} A_0 \\ B_0 \end{pmatrix} = - \begin{pmatrix} e^{ik2\pi} & 0 \\ 0 & e^{-ik2\pi} \end{pmatrix} \begin{pmatrix} A_n \\ B_n \end{pmatrix}. \tag{4.40}
$$

This system of equations admits a non-zero solution if and only if k is such that

$$
\det \left(\mathbb{I} + R_{\lambda_1} \begin{pmatrix} e^{-i\frac{k2\pi}{n}} & 0 \\ 0 & e^{i\frac{k2\pi}{n}} \end{pmatrix} R_{\lambda_2} \begin{pmatrix} e^{-i\frac{k2\pi}{n}} & 0 \\ 0 & e^{i\frac{k2\pi}{n}} \end{pmatrix} \dots R_{\lambda_n} \begin{pmatrix} e^{-i\frac{k2\pi}{n}} & 0 \\ 0 & e^{i\frac{k2\pi}{n}} \end{pmatrix} \right) = 0. \tag{4.41}
$$

It is convenient to define the polynomial

$$
P_{\boldsymbol{\lambda}}(z) = z^n \det \left(\mathbb{I} + R_{\lambda_1} \begin{pmatrix} 1/z & 0 \\ 0 & z \end{pmatrix} R_{\lambda_2} \begin{pmatrix} 1/z & 0 \\ 0 & -z \end{pmatrix} \dots R_{\lambda_n} \begin{pmatrix} 1/z & 0 \\ 0 & z \end{pmatrix} \right), \tag{4.42}
$$

of degree $2n$. This polynomial is palindromic, i.e. it satisfies $P_{\boldsymbol{\lambda}}(z) = z^{2n} P_{\boldsymbol{\lambda}}(1/z)$, and it has real coefficients. Let us call z_j, $j = 1, \dots, 2n$, the roots of that polynomial. When $\boldsymbol{\lambda} \in \mathbb{R}^n$, the roots lie on the unit circle $|z_j| = 1$. This corresponds to having real solutions for k in eq. (4.41). Therefore, in this case, we can write $z_j = e^{i\theta_j}$ with $\theta_j \in [0, 2\pi)$. Later, when we will analytically continue our result, the relation between z_j and θ_j will just be $\theta_j = -i \operatorname{Log} z_j$, without the property $\theta_j \in \mathbb{R}$.

The polynomial (4.42) can be rewritten in terms of its roots

$$
P_{\boldsymbol{\lambda}}(z) = \text{const.} \times \prod_{j=1}^{2n} (z - e^{i\theta_j(\boldsymbol{\lambda})}), \qquad \theta_j(\boldsymbol{\lambda}) \in [0, 2\pi), \tag{4.43}
$$

and each root determines a family of solutions to the quantization condition (4.41) for k via $z_j = e^{ik2\pi/n}$. The set of all such solutions is then

$$
\mathcal{S}_{\boldsymbol{\lambda}} = \bigcup_{j=1}^{2n} n \left(\mathbb{Z} + \frac{\theta_j(\boldsymbol{\lambda})}{2\pi} \right). \tag{4.44}
$$

Each $k \in \mathcal{S}_{\boldsymbol{\lambda}}$ defines a Bogoliubov mode

$$\eta_k = \int_0^{2\pi} \mathrm{d}x \left[u_k^*(x)\psi(x) + v_k^*(x)\bar{\psi}(x) \right], \tag{4.45}$$

which automatically satisfies $[H, \eta_k] = k\,\eta_k$ along with $(\eta_k)^\dagger = \eta_{-k}$, and the canonical anticommutation relations $\{\eta_k^\dagger, \eta_q\} = \delta_{k,q}$. Then the n-defect Hamiltonian (4.36) is diagonal in terms of them,

$$H = \frac{1}{2} \sum_{k \in \mathcal{S}_\lambda} k\eta_k^\dagger\eta_k, \tag{4.46}$$

where the sum runs over all the solutions k of eq. (4.41). Alternatively, one can write it as

$$H = \sum_{k \in \mathcal{S}_{\boldsymbol{\lambda}}^+} k(\eta_k\eta_{-k} - 1/2), \tag{4.47}$$

where the sum is now restricted to the set of positive solutions, $\mathcal{S}_{\boldsymbol{\lambda}}^+ = \{k \in \mathcal{S}_{\boldsymbol{\lambda}} | k > 0\}$. This expression is particularly convenient to compute the ground state energy.

4.3.2 Ground state energy

According to eq. (4.47), the ground state of the n-defect Hamiltonian (4.36) corresponds to the configuration with all the positive modes k occupied. Its energy is

$$E(\boldsymbol{\lambda}) = -\frac{1}{2} \sum_{k \in \mathcal{S}_{\boldsymbol{\lambda}}^+} k = -\frac{1}{2} \sum_{j=1}^{2n} \sum_{m=0}^{\infty} n\left(m + \frac{\theta_j}{2\pi}\right). \tag{4.48}$$

As in the $n = 1$ case above, these divergent series can be evaluated by zeta-regularization, using eq. (4.31),

$$E(\boldsymbol{\lambda}) = -\frac{n}{2} \sum_{j=1}^{2n} \zeta\left(-1, \frac{\theta_j}{2\pi}\right). \tag{4.49}$$

If we apply the identity $\zeta(-1, a) = \frac{1}{24} - \frac{(a - 1/2)^2}{2}$ for the Hurwitz zeta function, then we obtain

$$E(\boldsymbol{\lambda}) = \frac{n}{2} \sum_{j=1}^{2n} \left(\frac{1}{2}\left(\frac{\theta_j}{2\pi} - \frac{1}{2}\right)^2 - \frac{1}{24} \right). \tag{4.50}$$

This expression should be identified with the usual CFT formula for the ground state energy, $E = \Delta_n(\boldsymbol{\lambda}) - c/12$, with $c = 1/2$. Therefore, we find that for n equally-spaced defects the scaling dimension $\Delta_n(\boldsymbol{\lambda})$ is

$$\Delta_n(\boldsymbol{\lambda}) = -\frac{n^2 - 1}{24} + \frac{n}{4} \sum_{j=1}^{2n} \left(\frac{\theta_j}{2\pi} - \frac{1}{2}\right)^2. \tag{4.51}$$

This is the second main result of this paper section, which we will use to derive the Rényi entanglement asymmetry of the critical XY spin chain in the next section, where we also report the explicit expression of $\Delta_n(\boldsymbol{\lambda})$ for $n = 2$ and 3. As a first check of eq. (4.51), note that, when $\lambda_1 = \lambda_2 = \cdots = \lambda_n = 0$, we must obtain $\Delta_n(\boldsymbol{0}) = 0$. In fact, in that case, the polynomial (4.42) is $P_{\boldsymbol{\lambda}}(z) = (z^n + 1)^2$ and its roots are $z_j = e^{i2\pi\frac{j-1/2}{n}}$, $j = 1, \ldots, n$, all with multiplicity 2. Therefore, we have $\theta_j = \theta_{j+n} = 2\pi(j - 1/2)/n$ for $1 \leq j \leq n$. Inserting these roots in eq. (4.51) and performing the sum, we find $\Delta_n(\boldsymbol{0}) = 0$ as it should be.

4.4 Summary

For the convenience of the reader, let us briefly summarize the main result of this section. It is the second important result of this paper. It gives the exact scaling dimension $\Delta_n(\boldsymbol{\lambda})$ associated with the insertion of n-equally-spaced marginal defects in the massless Majorana fermion on a circle, with strengths $\lambda_1, \ldots, \lambda_n$. The result is given by eq. (4.51), which can also be rewritten in the form

$$\Delta_n(\boldsymbol{\lambda}) = -\frac{n^2 - 1}{24} + \frac{n}{4} \sum_{j=1}^{2n} \left(\frac{\mathrm{Log}(-z_j)}{2\pi i} \right)^2, \tag{4.52}$$

where $\mathrm{Log}(.)$ is the principal value of the logarithm, whose imaginary part takes values in $(-\pi, \pi]$ and its branch cut is taken along the negative real axis, and the z_j's $(j = 1, \ldots, 2n)$ are the $2n$ roots of the following polynomial of degree $2n$:

$$P_{\boldsymbol{\lambda}}(z) = z^n \det \left(\mathbb{I} + R_{\lambda_1} \begin{pmatrix} 1/z & 0 \\ 0 & z \end{pmatrix} R_{\lambda_2} \begin{pmatrix} 1/z & 0 \\ 0 & z \end{pmatrix} \ldots R_{\lambda_n} \begin{pmatrix} 1/z & 0 \\ 0 & z \end{pmatrix} \right), \tag{4.53}$$

with

$$R_\lambda = \begin{pmatrix} \cosh \lambda & \sinh \lambda \\ \sinh \lambda & \cosh \lambda \end{pmatrix}. \tag{4.54}$$

We have derived this result for defect strengths $\lambda_j \in \mathbb{R}$, but it can be analytically continued to $\lambda_j \in \mathbb{C}$. In particular, in what follows, we will take $\lambda_j \to i\alpha_j$ to derive the Rényi entanglement asymmetry in the critical XY spin chain.

## 5 Rényi entanglement asymmetry in the critical XY spin chain

In this section, we derive the asymptotic behavior of the Rényi entanglement asymmetry in the ground state of the critical XY spin chain using the results obtained above. At the critical lines $\gamma \neq 0$, $|h| = 1$, the charged moments $\mathcal{Z}_n(\boldsymbol{\alpha})$ behave as in eq. (2.18) for large subsystem length ℓ. While the string tension $T_n(\boldsymbol{\alpha})$ is given by eq. (3.3), we have found in section 4.3 that the scaling dimension $\tilde{\Delta}_n(\boldsymbol{\alpha})$ can be obtained, upon the analytic continuation $\boldsymbol{\lambda} = i\boldsymbol{\alpha}$, from eq. (4.52), which further requires to determine the roots of the polynomial (4.53). Unfortunately, we are not able to find a general expression for these roots. Here we first consider the cases $n = 2$ and 3, and we check our analytic prediction for $\mathcal{Z}_n(\boldsymbol{\alpha})$ against exact numerical results in the ground state of the XY spin chain. We then derive by applying the saddle point approximation discussed in section 2.2.3 the asymptotic behavior of the Rényi entanglement asymmetry for any integer index n, and by analytically continuing it, the replica limit $n \to 1$.

5.1 Numerical checks

5.1.1 $n = 2$ charged moments

In the case of two defects located at the points indicated in the left panel of figure 5, the polynomial of eq. (4.42) reads

$$P_{\boldsymbol{\lambda}}(z) = \cosh \lambda_1 \cosh \lambda_2 (1 + z^4) + 2(1 + \sinh \lambda_1 \sinh \lambda_2) z^2. \tag{5.1}$$
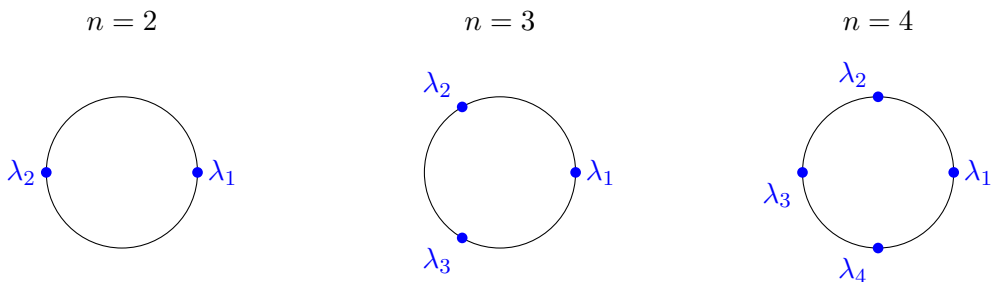
Figure 5. Disposition of the point defects on the circle in the calculation of the charged moments $\mathcal{Z}_n(\boldsymbol{\alpha})$ for $n = 2, 3$ and 4. The circle has length 2π and the defect of strength λ_j is located at the point $x_j = \frac{2\pi j}{n}$.

It is a bit cumbersome to write the roots explicitly, but using them in eq. (4.52) we arrive at the formula for the scaling dimension associated with the insertion of two defects

$$\Delta_2(\lambda_1, \lambda_2) = \frac{1}{2\pi^2} \left[\arctan\left(\tanh\frac{\lambda_1}{2}\right) - \arctan\left(\tanh\frac{\lambda_2}{2}\right) \right]^2. \tag{5.2}$$

To keep formulas compact, here we write the roots only in the special case $\lambda_2 = -\lambda_1 = \lambda$, which is the case that we use below in our analysis of the asymmetry. In that case the four roots are:

$$z = \pm\frac{i \pm \sinh\lambda}{\cosh\lambda}, \tag{5.3}$$

and, taking $\theta = -i\log z$, their arguments are

$$\theta_1 = \pi - \theta_2 = 2\arctan\tanh(\lambda/2) + \frac{\pi}{2}, \tag{5.4}$$

$$\theta_3 = 3\pi - \theta_4 = 2\arctan\tanh(\lambda/2) + \frac{3\pi}{2}. \tag{5.5}$$
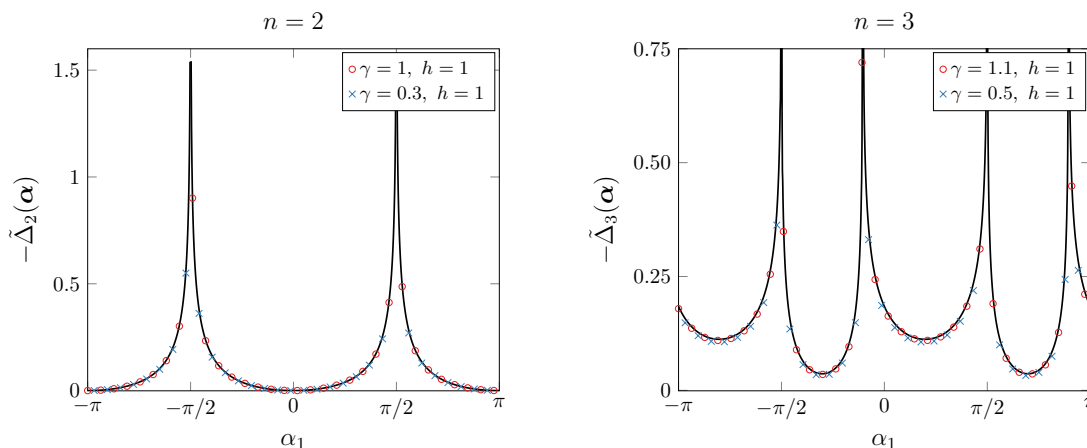
Plugging them in eq. (4.52), we obtain

$$\Delta_2(\lambda, -\lambda) = \frac{2}{\pi^2} \arctan^2\left(\tanh\frac{\lambda}{2}\right) \tag{5.6}$$

and, taking the analytic continuation $\lambda = i\alpha$,

$$\tilde{\Delta}_2(\alpha, -\alpha) = -\frac{2}{\pi^2} \operatorname{arctanh}^2\left(\tan\frac{\alpha}{2}\right). \tag{5.7}$$

Note that, in eq. (5.7), $\tilde{\Delta}_2(\alpha, -\alpha)$ is only well-defined in the interval $\alpha \in (-\pi/2, \pi/2)$ since the domain of definition of $\operatorname{arctanh}(x)$ is $x \in (-1, 1)$. On the other hand, the ground state of the critical XY spin chain is invariant under the subgroup $\mathbb{Z}_2 \subset \mathrm{U}(1)$ of spin flips, which implies that the charged moments $\mathcal{Z}_2(\boldsymbol{\alpha})$ are periodic $\mathcal{Z}_2(\boldsymbol{\alpha} + \boldsymbol{\pi}) = \mathcal{Z}_2(\boldsymbol{\alpha})$. Therefore, eq. (5.7) must be extended outside the interval $\alpha \in (-\pi/2, \pi/2)$ such that this periodicity is satisfied,

$$\tilde{\Delta}_2(\alpha, -\alpha) = \begin{cases} -\frac{2}{\pi^2} \operatorname{arctanh}^2\left(\tan\frac{\alpha}{2}\right), & \alpha \in (-\pi/2, \pi/2), \\ -\frac{2}{\pi^2} \operatorname{arctanh}^2\left(\tan\frac{(\pi-\alpha)}{2}\right), & \alpha \in (-\pi, -\pi/2) \cup (\pi/2, \pi). \end{cases} \tag{5.8}$$

Figure 6. Scaling dimension $\tilde{\Delta}_n(\boldsymbol{\alpha})$ for two (left panel) and three (right panel) defects, which appears in the asymptotic behavior of the charged moments $\mathcal{Z}_n(\boldsymbol{\alpha})$. For $n = 2$, we take $\alpha_2 = -\alpha_1$ and we vary α_1. For $n = 3$, we set $\alpha_1 + \alpha_2 + \alpha_3 = 0$ and change α_1 with $\alpha_2 = 1.9$. The symbols have been obtained numerically as detailed in the main text for the ground state of the XY spin chain along the critical line $\gamma > 0$ and $h = 1$. The curves are the CFT prediction (4.52), that for $n = 2$ simplifies to (5.8).

In the left panel of figure 6, we numerically check this result. As we explain in appendix C, the charged moments $\mathcal{Z}_n(\boldsymbol{\alpha})$ can be exactly calculated numerically in the ground state of the critical XY spin chain with eq. (C.4). Using this expression together with eq. (3.3), we compute $\log(\mathcal{Z}_2(\boldsymbol{\alpha})e^{T_2(\boldsymbol{\alpha})\ell})$ with $\boldsymbol{\alpha} = (\alpha, -\alpha)$ for a fixed α and $\ell = 50, 60, \ldots, 100$ and we fit the curve $-\tilde{\Delta}_2(\boldsymbol{\alpha}) \log \ell + \text{const.}$ to this set of points. In the plot on the left side of figure 6, the symbols correspond to the values of $\tilde{\Delta}_2(\boldsymbol{\alpha})$ obtained in the fit for different angles α and couplings $(h = 1, \gamma)$, while the solid curve is the prediction of eq. (5.8). We obtain a very good agreement between them.

The divergence of $\tilde{\Delta}_2(\boldsymbol{\alpha})$ in $\boldsymbol{\alpha} = (\pm\pi/2, \mp\pi/2)$ does not mean that the charged moment is divergent itself but that the charged moment has a different scaling in ℓ. We numerically observe that in this case the scaling is $\log \mathcal{Z}_2(\boldsymbol{\alpha}) = -T(\boldsymbol{\alpha})\ell + O\left((\log \ell)^2\right)$. In general, we observe this anomalous scaling with a $(\log \ell)^2$ term in the charged moment $\mathcal{Z}_n(\boldsymbol{\alpha})$ for every n when at least one α_j is equal to $\pi/2$. Being these points a measure zero set in the integral for the asymmetry, the analysis performed in section 2.2.3 does not change.
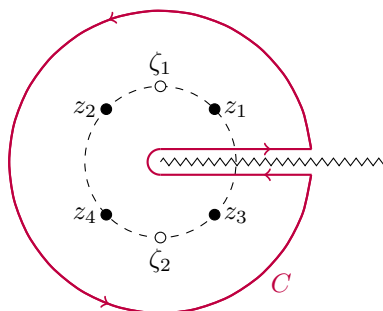
5.1.2 $n = 3$ charged moments

For three defects at the positions of the middle panel of figure 5 on a circle, the polynomial (4.42) is

$$P_{\boldsymbol{\lambda}}(z) = C_{\boldsymbol{\lambda}} + S_{\boldsymbol{\lambda}}z^2 + 2z^3 + S_{\boldsymbol{\lambda}}z^4 + C_{\boldsymbol{\lambda}}z^6, \tag{5.9}$$

with

$$C_{\boldsymbol{\lambda}} = \cosh \lambda_1 \cosh \lambda_2 \cosh \lambda_3, \quad S_{\boldsymbol{\lambda}} = \sinh \lambda_1 \sinh \lambda_2 \cosh \lambda_3 + \text{cycl. perm.} \tag{5.10}$$

To compute the coefficient $\tilde{\Delta}_3(\boldsymbol{\alpha})$ that enters in the asymptotic behavior of the charged moment $\mathcal{Z}_3(\boldsymbol{\alpha})$, we have to impose $\lambda_1 + \lambda_2 + \lambda_3 = 0$ due to the Dirac delta in eq. (2.8).

Figure 7. Schematic representation of the contour integral that gives the scaling dimension $\Delta_n(\boldsymbol{\lambda})$ for the case $n = 2$. The zig-zag line is the branch cut $[0, \infty)$ of the function $\mathrm{Log}(z)$. The filled black dots are the roots z_j of the polynomial $P_{\boldsymbol{\lambda}}(z)$ and the white ones represent the poles of the integrand in eq. (5.16), after expanding quadratically $P_{\boldsymbol{\lambda}}(z)$ in $\boldsymbol{\lambda}$.

In that case, $S_{\boldsymbol{\lambda}} = 1 - C_{\boldsymbol{\lambda}}$ and the polynomial has two equal roots $z_1 = z_2 = -1$. The other four roots are

$$
\begin{aligned}
z_3 = z_4^* &= \frac{\sqrt{C_{\boldsymbol{\lambda}}} + \sqrt{C_{\boldsymbol{\lambda}} - 1} \pm i\sqrt{1 + 2C_{\boldsymbol{\lambda}} - 2\sqrt{C_{\boldsymbol{\lambda}}(C_{\boldsymbol{\lambda}} - 1)}}}{2\sqrt{C_{\boldsymbol{\lambda}}}}, \\
z_5 = z_6^* &= \frac{\sqrt{C_{\boldsymbol{\lambda}}} - \sqrt{C_{\boldsymbol{\lambda}} - 1} \pm i\sqrt{1 + 2C_{\boldsymbol{\lambda}} + 2\sqrt{C_{\boldsymbol{\lambda}}(C_{\boldsymbol{\lambda}} - 1)}}}{2\sqrt{C_{\boldsymbol{\lambda}}}}.
\end{aligned}
\tag{5.11}
$$

Plugging them in eq. (4.52) and performing the analytic continuation $\boldsymbol{\lambda} = i\boldsymbol{\alpha}$, we obtain the analytic expression for $\tilde{\Delta}_3(\boldsymbol{\alpha})$. We numerically check it in the right panel of figure 6 as we have done for the case $n = 2$. We can calculate the exact value of the charged moment $\mathcal{Z}_3(\boldsymbol{\alpha})$ in the critical XY spin chain employing eq. (C.4) in the appendix. Combining it with eq. (3.3), we compute $\log(\mathcal{Z}_3(\boldsymbol{\alpha})e^{\ell T_3(\boldsymbol{\alpha})})$ for a given $\boldsymbol{\alpha} = (\alpha_1, \alpha_2, -\alpha_1 - \alpha_2)$ and $\ell = 50, 60, \ldots, 100$. With the resulting set of points, we fit the function $-2\tilde{\Delta}_3(\boldsymbol{\alpha})/3 \log \ell + \mathrm{const}$. In the plot on the right side of figure 6, the symbols represent the coefficient $\tilde{\Delta}_3(\boldsymbol{\alpha})$ that we get in the fit in terms of α for different couplings $(h = 1, \gamma)$ and the curve is the CFT prediction of eq. (4.52) using the roots (5.11). The agreement is excellent.

5.2 Asymptotic behavior of the entanglement asymmetry

We now compute the asymptotic behavior of the entanglement asymmetry for large subsystem size ℓ applying the general result (2.30). As we have seen in section 3, for the U(1) group that we are considering we have $\mathrm{vol}\, G = 2\pi$, $\dim G = 1$, $\mu(0) = 1$, and the symmetric subgroup H is the $\mathbb{Z}_2$ spin-flip symmetry. The string tension $T_n(\boldsymbol{\alpha})$ is given by eq. (3.3), $\mathsf{H}_t = t''(0)$, and, according to eq. (3.6), $t''(0) = \gamma/(2(1 + \gamma))$ at the critical lines $|h| = 1$. Since $\dim G = 1$, the matrices D_p, defined in eq. (2.24), that enter in the calculation of the coefficient b_n of the $\log \ell/\ell$ term are scalars and correspond to the eigenvalues ν_p of the Hessian matrix of the scaling dimension $\Delta_n(\boldsymbol{\lambda})$,

$$
(\mathsf{H}_{\Delta_n})_{ab} = \left(\frac{\partial^2 \Delta_n(\boldsymbol{\lambda})}{\partial \lambda_a \partial \lambda_b} \right)_{\boldsymbol{\lambda} = \mathbf{0}}, \quad a, b = 1, \ldots, n,
\tag{5.12}
$$

such that $\mathsf{D}_p = -2\nu_p/n$ (recall that in our case $\beta_n(\boldsymbol{\alpha}) = \frac{2}{n}\Delta_n(i\boldsymbol{\alpha})$). Therefore, eq. (2.30) reads in this case as

$$\Delta S_A^{(n)} = \frac{1}{2}\log\ell + a_n + b_n\frac{\log\ell}{\ell} + \cdots \tag{5.13}$$

with

$$a_n = \frac{1}{2}\log\frac{\pi t''(0)n^{\frac{1}{n-1}}}{2} \tag{5.14}$$

and

$$b_n = \frac{1}{n(1-n)t''(0)}\sum_{p=1}^{n-1}\nu_p. \tag{5.15}$$

5.2.1   The Hessian of $\boldsymbol{\Delta_n(\lambda)}$

The only missing ingredient are the eigenvalues ν_p of the Hessian (5.12) of the scaling dimension $\tilde{\Delta}_n(\boldsymbol{\alpha})$. To calculate the latter, it is convenient to rewrite eq. (4.52) as a contour integral using the residue theorem,

$$\Delta_n(\boldsymbol{\lambda}) = \frac{1}{2\pi i}\oint_C dz f_n(z)\frac{d}{dz}\mathrm{Log}\, P_{\boldsymbol{\lambda}}(z), \tag{5.16}$$

with

$$f_n(z) = -\frac{n^2-1}{48\,n} + \frac{n}{4}\left(\frac{i\,\mathrm{Log}(-z)}{2\pi}\right)^2. \tag{5.17}$$

The polynomial $P_{\boldsymbol{\lambda}}(z)$ is defined in eq. (4.53). The contour C encircles all the roots of $P_{\boldsymbol{\lambda}}(z)$ as we depict in figure 7, leaving the branch cut of $\mathrm{Log}(z)$ outside of the region that it delimits. The advantage of this approach is that we can easily calculate the second derivatives of $\Delta_n(\boldsymbol{\lambda})$ at $\boldsymbol{\lambda} = \boldsymbol{0}$ by expanding quadratically the polynomial $P_{\boldsymbol{\lambda}}(z)$ around this point. If we rewrite (4.53) in the form

$$P_{\boldsymbol{\lambda}}(z) = z^n\left\{2 + \mathrm{tr}\left[R_{\lambda_1}\begin{pmatrix}1/z & 0\\0 & z\end{pmatrix}\ldots R_{\lambda_n}\begin{pmatrix}1/z & 0\\0 & z\end{pmatrix}\right]\right\}, \tag{5.18}$$

then it is easy perform the expansion,

$$P_{\boldsymbol{\lambda}}(z) = P_0(z)\left[1 + \frac{1}{2}\sum_{a,b=1}^{n}\lambda_a\lambda_b\frac{z^{2n-2|b-a|} + z^{2|b-a|}}{(z^n+1)^2}\right] + O(\lambda^3), \tag{5.19}$$

where $P_0(z) = (z^n+1)^2$. If we plug it in the contour integral (5.16) and we integrate by parts, we find

$$\Delta_n(\boldsymbol{\lambda}) = -\frac{1}{2}\sum_{a,b=1}^{n}\lambda_a\lambda_b\oint_C\frac{dz}{2\pi i}\frac{df_n(z)}{dz}\frac{z^{2(n-|b-a|)} + z^{2|b-a|}}{(z^n+1)^2} + O(\lambda^3), \tag{5.20}$$

and

$$\frac{df_n(z)}{dz} = -\frac{n}{8\pi^2}\frac{\mathrm{Log}(-z)}{z}. \tag{5.21}$$

Observe that, according to this result, $\Delta_n(\boldsymbol{\lambda}) = 0$, as expected. Therefore, the components of the Hessian of $\Delta_n(\boldsymbol{\lambda})$ can be identified with

$$(\mathsf{H}_{\Delta_n})_{ab} = -\oint_C \frac{\mathrm{d}z}{2\pi i} \frac{\mathrm{d}f_n(z)}{\mathrm{d}z} \frac{z^{2(n-|b-a|)} + z^{2|b-a|}}{(z^n+1)^2}. \tag{5.22}$$

Given that $0 \le |b-a| \le n-1$, the numerator of the integrand above is, up to the $\mathrm{Log}(z)$ factor, a polynomial. Since the cut of the logarithm lies outside the region enclosed by C, then the only singularities the contribute to the integral are the zeros of $z^n + 1$ in the denominator, $\zeta_j = e^{i\frac{2\pi}{n}(j-\frac{1}{2})}$, $j = 1, \ldots, n$. Applying the residue theorem, we have

$$(\mathsf{H}_{\Delta_n})_{ab} = \frac{n}{8\pi^2} \sum_{j=1}^n \mathrm{res}\left[\frac{\mathrm{Log}(-z)}{z} \frac{z^{2(n-|b-a|)} + z^{2|b-a|}}{(z^n+1)^2}, \ \zeta_j\right]. \tag{5.23}$$

These residues can be evaluated explicitly,

$$\mathrm{res}\left[\frac{z^{p-1}\,\mathrm{Log}(-z)}{(z^n+1)^2}, \ \zeta_j\right] = \frac{\zeta_j^p}{n^2}\left(1 + (p-n)\frac{i\pi(2j-n-1)}{n}\right).$$

After summing them in eq. (5.23), we eventually find that the Hessian of $\Delta_n(\boldsymbol{\alpha})$ is a circulant matrix,

$$(\mathsf{H}_{\Delta_n})_{ab} = c_{a-b}, \quad \text{with} \quad c_l = \frac{1}{4\pi^2} \times \begin{cases} 1, & \text{if} \quad l = 0, \\ \frac{2\pi}{n}\frac{l-n/2}{\sin(\frac{2\pi}{n}l)}, & \text{if} \quad l = 1, \ldots, n-1, \end{cases} \tag{5.24}$$

as a consequence of the symmetry under the cyclic exchange of the replicas.

5.2.2 Application to the asymmetry

According to eq. (5.15), the coefficient of the $\log \ell / \ell$ term in the asymmetry is given by the eigenvalues ν_p of the Hessian H_{Δ_n}. In our case, since the it is a circulant matrix, the eigenvalues are given by the Fourier transform of its entries,

$$\nu_p = \sum_{l=0}^{n-1} c_l e^{i\frac{2\pi p l}{n}}. \tag{5.25}$$

Combining eqs. (5.15) and (5.25), and doing carefully the sums, we find that

$$b_n = \frac{\gamma+1}{2\gamma} \times \begin{cases} \dfrac{1}{(1-n)\pi^2} + \dfrac{1}{n(n-1)\pi}\displaystyle\sum_{l=1}^{n/2-1} \csc\left(\frac{2\pi l}{n}\right), & n \text{ even}, \\[3ex] -\dfrac{1}{n\pi^2} - \dfrac{1}{n^2(n-1)\pi}\displaystyle\sum_{l=1}^{n-1}(n-2l)\csc\left(\frac{2\pi l}{n}\right), & n \text{ odd}, \end{cases} \tag{5.26}$$

where we have taken into account that $t''(0) = \gamma/(2(\gamma+1))$. This result can be analytically continued to non integer values of n by using the integral representation of the cosecant function

$$\csc(\pi z) = \frac{1}{\pi}\int_0^\infty \mathrm{d}x\, \frac{x^z}{x^2+x}. \tag{5.27}$$

Applying it in eq. (5.26) for n even, we find

$$b_n = -\frac{\gamma+1}{2\gamma}\left[\frac{1}{(n-1)\pi^2} + \frac{1}{n(n-1)\pi^2}\int_0^\infty \frac{\mathrm{d}x}{x(x+1)}\frac{x^{2/n}-x}{1-x^{2/n}}\right]. \tag{5.28}$$

It turns out this expression reproduces the exact values of the coefficient b_n for n odd as well, so eqs. (5.26) and (5.28) are equivalent expressions for all integer n.

Eqs. (5.26)-(5.28) are the third main result of this paper: we have arrived at the exact expression for the coefficient b_n of the $\log\ell/\ell$ term in the Rényi entanglement asymmetry of the XY spin chain at criticality.

Finally, taking the replica limit $n \to 1$ in eq. (5.28), we find that the coefficient for the (von Neumann) entanglement asymmetry is

$$\lim_{n\to 1} b_n = -\frac{4+\pi^2}{16\pi^2}\frac{\gamma+1}{\gamma}. \tag{5.29}$$

Thus, our final result is that the entanglement asymmetry at criticality in the XY spin chain is

$$\Delta S_A = \frac{1}{2}\log\ell + \frac{1}{2}\log\frac{\pi\gamma}{4(1+\gamma)} + \frac{1}{2} - \frac{4+\pi^2}{16\pi^2}\frac{\gamma+1}{\gamma}\frac{\log\ell}{\ell} + \cdots \tag{5.30}$$

We stress once again that what is remarkable here is the $\log\ell/\ell$ term, which only appears in critical systems. We also stress that the 'semi-universality' of b_n (in the sense of ref. [75]) is manifest here, because it depends on the parameter γ of the XY Hamiltonian. A truly universal quantity —such as, for instance, the scaling dimension $\Delta_n(\boldsymbol{\lambda})$ — would depend only on the CFT data and not on the details of the underlying microscopic model, so it would not depend on γ.

6 Conclusions

In this paper, we have analyzed the entanglement asymmetry in one dimensional critical extended quantum systems using CFT methods. This observable measures how much a symmetry is broken in a part of the system. Applying the replica trick, it can be obtained from the charged moments of the subsystem's reduced density matrix. We have seen that, in the ground state of a 1+1 dimensional quantum field theory, using the correspondence between the unitary operators that represent the symmetry group in the Hilbert space and defect lines in the path integral approach, the charged moments can be identified with a quotient of the partition functions of the theory on a Riemann surface with and without defect lines inserted along each branch cut. When the state respects the symmetry, the defects are topological and any deformation leaves the partition function invariant, yielding a zero asymmetry. In this formulation, the entanglement asymmetry can be interpreted as a measure of how much the defects are non topological. Utilizing well-known scaling arguments for the partition function in two dimensions, we have deduced the asymptotic behavior of the charged moments that provide the entanglement asymmetry. While for non critical systems the moments decay exponentially with the subsystem size, see refs. [3, 4, 13], in the critical case we have found that they contain an extra algebraic factor. The coefficient

of the exponential decaying term can be interpreted as the line tension of the defects and is non-universal; that is, it depends on the specific lattice realization of the field theory. The exponent of the algebraic factor is universal and, therefore, it is fully determined by the CFT that describes the critical point and depends on the properties of the defects associated with the symmetry group. From this result, we have derived the asymptotic behavior of the ground state entanglement asymmetry for a generic compact Lie group. Both for non-critical and critical systems, it grows at leading order logarithmically with the subsystem size ℓ and a coefficient proportional to the dimension of the Lie group. Criticality yields a $\log \ell/\ell$ correction, which is semi-universal as its coefficient depends not only on the universal exponent of the charged moments but also on the defect tension.

In the rest of the paper, we have specialized to the ground state of the XY spin chain, which explicitly breaks the U(1) symmetry of spin rotations around the transverse axis. The charged moments and the entanglement asymmetry of this model have been investigated outside the critical lines in ref. [4] employing lattice methods. Here we have considered the critical lines described by the massless Majorana fermion theory in the scaling limit, after fermionizing it with a Jordan-Wigner transformation. In this case, the defect lines correspond to a marginal deformation of this CFT. Exploiting conformal invariance, the universal exponent that appears in the charged moments can be identified with the ground state energy of the massless Majorana fermion theory on a circle with equi-spaced marginal point defects of different strength. To obtain it, we have carefully diagonalized its Hamiltonian for an arbitrary number of defects. Combining this result with those found in ref. [4] for the non-universal exponential term, we have obtained an analytic expression for the entanglement asymmetry.

A crucial point in our problem is that the defects we are considering are marginal, which makes non-trivial the dependence of the CFT partition function on them. As we have already emphasized, the partition function hinges on the specific CFT and symmetry group under study. Therefore, it would be desirable to consider other models and symmetries; for example, the SU(2) group of spin rotations in the critical XXZ spin chain, whose continuum limit is the massless compact boson. The correspondence between global symmetries and (topological) defect lines that we exploit here can be enlarged to encompass higher-form symmetries [17], symmetries generated by extended operators supported not only on lines but also on higher dimensional manifolds, and non-invertible symmetries [82, 83], which lack of an inverse element. It would be interesting to explore if the notion of entanglement asymmetry can be extended to these generalized symmetries.

Acknowledgments

A Fermionization and continuum limit of the XY spin chain

The fermionization of the XY spin chain is performed with the Jordan-Wigner transformation [84]. For completeness, we present it in multiple steps. First we map the spin chain to a model with complex lattice fermions, the Kitaev chain. Then we further map the system to lattice Majorana fermions. Finally, we take the continuum limit and get the Majorana CFT.

We consider the XY spin chain, writing explicitly the ferromagnetic coupling J. While in the main text this is set to $J = 1$, here is important to have it in order to perform the continuum limit carefully. The Hamiltonian then is

$$H_{\mathrm{XY}} = -\frac{J}{2} \sum_{j \in \mathbb{Z}} \left(\frac{1 + \gamma}{2} \sigma_j^x \sigma_{j+1}^x + \frac{1 - \gamma}{2} \sigma_j^y \sigma_{j+1}^y + h \sigma_j^z \right). \tag{A.1}$$

Kitaev chain. The Jordan-Wigner transformation is

$$\sigma_j^x = e^{i\pi \sum_{l<j} c_j^\dagger c_j} \left(c_j^\dagger + c_j \right), \qquad \sigma_j^x = e^{i\pi \sum_{l<j} c_j^\dagger c_j} i \left(c_j^\dagger - c_j \right), \qquad \sigma_j^z = 1 - 2c_j^\dagger c_j, \tag{A.2}$$

and the operators c_j, $c_j^\dagger$ satisfy the anticommutation relations $\{c_j, c_l\} = 0$ and $\{c_j, c_l^\dagger\} = \delta_{jl}$. Then the Hamiltonian (3.1) of the XY model is mapped to the Hamiltonian of the Kitaev chain

$$H_{\mathrm{Kit}} = -\frac{J}{2} \sum_{j \in \mathbb{Z}} \left[c_j^\dagger c_{j+1} + c_{j+1}^\dagger c_j + \gamma \left(c_j^\dagger c_{j+1}^\dagger + c_{j+1} c_j \right) + h \left(1 - 2c_j^\dagger c_j \right) \right] \tag{A.3}$$

and the charge Q_A for $A = \{1, \dots, \ell\}$ becomes $Q_A = \sum_{j \in A} c_j^\dagger c_j$.

It is well known that the XY model flows in the infra-red to the Ising CFT for $h = 1$, $\gamma \in \mathbb{R}$. Thus all these points in the parameter space belong to the same universality class. For simplicity, we consider the case $h = \gamma = 1$.

Majorana chain. Each pair of complex fermion operators c_j, $c_j^\dagger$ can be split in the following pair of Majorana operators

$$c_j^\dagger = \frac{1}{2} \left(a_{2j} + i a_{2j+1} \right), \qquad\qquad c_j = \frac{1}{2} \left(a_{2j} - i a_{2j+1} \right), \tag{A.4}$$

which satisfy the algebra $a_j^\dagger = a_j$ and $\{a_j, a_j\} = 2\delta_{jl}$. Then the Hamiltonian becomes

$$H_{\mathrm{Maj}} = \frac{iJ}{2} \sum_{j \in \mathbb{Z}} a_{j+1} a_j \tag{A.5}$$

and the charge

$$Q_A = \frac{1}{2} \sum_{j \in A} \left(1 + i a_{2j+1} a_{2j} \right). \tag{A.6}$$

Continuum limit. The continuum limit is performed by first defining the following new Majorana lattice operators ψ_j, $\bar{\psi}_j$

$$a_{2j} = \psi_j + \bar{\psi}_j, \qquad\qquad a_{2j+1} = \psi_j - \bar{\psi}_j, \tag{A.7}$$

which form two anticommuting families of Majorana fermions, with algebra

$$\{\psi_j, \psi_l\} = \delta_{jl}, \qquad \{\bar{\psi}_j, \bar{\psi}_l\} = \delta_{jl}, \qquad \{\psi_j, \bar{\psi}_l\} = 0. \qquad (A.8)$$

The Hamiltonian in these variables reads

$$H_{\text{Maj}'} = \frac{iJ}{2} \sum_{j \in \mathbb{Z}} \left(2\psi_j \bar{\psi}_j + \psi_j \psi_{j-1} + \bar{\psi}_j \psi_{j-1} - \psi_j \bar{\psi}_{j-1} - \bar{\psi}_j \bar{\psi}_{j-1} \right) \qquad (A.9)$$

and the charge

$$Q_A = \frac{1}{2} \sum_{j \in A} \left(1 + i2\psi_j \bar{\psi}_j \right). \qquad (A.10)$$

Finally, we perform the continuum limit. We call the continuum variable $x \in \mathbb{R}$ and introduce a lattice spacing s so that

$$\psi_j \simeq \frac{\psi(x)}{\sqrt{s}}, \qquad \psi_{j-1} \simeq \frac{\psi(x-s)}{\sqrt{s}} \simeq \frac{1}{\sqrt{s}}(\psi(x) - s\partial_x \psi(x)). \qquad (A.11)$$

The continuum fields satisfy the algebra $\{\psi(x), \psi(y)\} = \delta(x-y)$, $\{\bar{\psi}(x), \bar{\psi}(y)\} = \delta(x-y)$, $\{\psi(x), \bar{\psi}(y)\} = 0$. The Hamiltonian becomes

$$H = \frac{J'}{2i} \int_{\mathbb{R}} \mathrm{d}x \left[\psi(x)\partial_x \psi(x) - \bar{\psi}(x)\partial_x \bar{\psi}(x) \right], \qquad (A.12)$$

where J' is the continuum version of J, given by $J' = Js$ in the limit $s \to 0$ and $J \to \infty$. Deriving the equations of motion for ψ and $\bar{\psi}$, J' can be recognized to be the sound velocity, which we set to 1. Finally, the charge operator, discarding the constant term in eq. (A.10) that acts trivially on the Hilbert space, becomes

$$Q_A = i \int_A \psi(x)\bar{\psi}(x) \,\mathrm{d}x. \qquad (A.13)$$

B Defects in the Hamiltonian formalism

In this appendix, we consider a massless Majorana fermion on a line, with a defect implemented as a localized mass term

$$H_\mu = \frac{1}{2i} \int_{\mathbb{R}} (\psi\partial_x\psi - \bar{\psi}\partial_x\bar{\psi}) \,\mathrm{d}x - i\mu\, \psi(0)\bar{\psi}(0), \qquad \mu \in \mathbb{R}. \qquad (B.1)$$

We show that this formulation is equivalent to the one given in the main text, where the defect is only encoded in the gluing conditions. We provide the explicit relation between the defect strength μ and the gluing parameter λ. We find that if the defect term in the Hamiltonian is Hermitian, then λ has to be real. This is a further justification of the analytic continuation $\alpha \mapsto -i\lambda$ that is performed in the main text.

We have the following commutators

$$[H_\mu, \psi(x)] = i\partial_x\psi(x) + i\mu\delta(x)\bar{\psi}(0), \qquad (B.2)$$

$$\left[H_\mu, \bar{\psi}(x)\right] = -i\partial_x\bar{\psi}(x) - i\mu\delta(x)\psi(0). \qquad (B.3)$$

To relate this to gluing conditions at the origin, we can look for eigenmodes of that Hamiltonian of the form

$$\eta_k = \int_{\mathbb{R}} \left[u_k^*(x)\psi(x) + v_k^*(x)\bar{\psi}(x) \right] \mathrm{d}x, \tag{B.4}$$

with

$$u_k(x) = \begin{cases} A_0 e^{ikx}, & x < 0, \\ A_1 e^{ikx}, & x > 0, \end{cases} \qquad v_k(x) = \begin{cases} B_0 e^{-ikx}, & x < 0, \\ B_1 e^{-ikx}, & x > 0, \end{cases} \tag{B.5}$$

for some constants A_0, A_1, B_0, B_1. This Ansatz gives the following commutator with the Hamiltonian,

$$[H_\mu, \eta_k] = k\eta_k - i\left(A_0^* - A_1^* - \frac{\mu}{2}(B_0^* + B_1^*) \right)\psi(0) + i\left(B_0^* - B_1^* - \frac{\mu}{2}(A_0^* + A_1^*) \right)\bar{\psi}(0). \tag{B.6}$$

We see that η_k is a Bogoliubov mode with energy k if the last two terms vanish. This gives the constraint

$$\begin{pmatrix} A_0 \\ B_0 \end{pmatrix} = \begin{pmatrix} \frac{1+\mu^2/4}{1-\mu^2/4} & \frac{\mu}{1-\mu^2/4} \\ \frac{\mu}{1-\mu^2/4} & \frac{1+\mu^2/4}{1-\mu^2/4} \end{pmatrix} \begin{pmatrix} A_1 \\ B_1 \end{pmatrix}. \tag{B.7}$$

Thus, we recover the gluing condition (4.7) with the matrix (4.13) obtained after the analytic continuation of the gluing parameter, provided that

$$\frac{\mu}{2} = \tanh\left(\frac{\lambda}{2} \right). \tag{B.8}$$

C Numerical calculation of the charged moments

In this appendix, we report the formulae that we employ to compute numerically the charged moments (2.9) for the U(1) group of spin rotations around the z axis in the ground state of the XY spin chain (3.1). As we show in appendix A, this model maps into a quadratic fermionic chain after the Jordan-Wigner transformation (A.2). Therefore, its ground state satisfies Wick theorem. This implies that the reduced density matrix ρ_A of a single interval A of length ℓ is Gaussian and it is fully determined by the $2\ell \times 2\ell$ two-point fermionic correlation matrix [85]

$$\Gamma_{jj'} = 2\mathrm{tr}\left[\rho_A \begin{pmatrix} c_j \\ c_j^\dagger \end{pmatrix} (c_{j'}^\dagger, c_{j'}) \right] - \delta_{jj'}, \tag{C.1}$$

with $j, j' = 1, \ldots, \ell$. For the ground state of the XY spin chain, its entries are

$$\Gamma_{jj'} = \int_0^{2\pi} \frac{\mathrm{d}k}{2\pi} \mathcal{G}(k) e^{-ik(j-j')}, \tag{C.2}$$

where $\mathcal{G}(k)$ is the 2×2 matrix

$$\mathcal{G}(k) = \begin{pmatrix} \cos\xi_k & -i\sin\xi_k \\ i\sin\xi_k & -\cos\xi_k \end{pmatrix} \tag{C.3}$$

and $\cos\xi_k$, $\sin\xi_k$ are given in eq. (3.4).

After the Jordan-Wigner transformation, the transverse magnetization (3.2) that generates the U(1) symmetry is also quadratic and, consequently, Gaussian. Therefore, the charged moments $\mathcal{Z}_n(\boldsymbol{\alpha})$ are the trace of a product of Gaussian operators. Using the well-known properties of this kind of operators, the charged moments can be calculated in terms of the two-point correlataion matrix Γ as

$$\mathcal{Z}_n(\boldsymbol{\alpha}) = \sqrt{\det\left[\left(\frac{I - \Gamma}{2}\right)^n \left(I + \prod_{j=1}^{n} W_j\right)\right]}, \qquad \text{(C.4)}$$

where $W_j = (I + \Gamma)(I - \Gamma)^{-1}e^{i\alpha_{j,j+1}n_A}$ and n_A is a diagonal matrix with $(n_A)_{2j,2j} = 1$, $(n_A)_{2j-1,2j-1} = -1$, $j = 1, \cdots, \ell$. The detailed derivation of this expression can be found in ref. [7]. We use it to obtain the exact numerical values of the charged moments in the plots of figure 6.

Open Access. This article is distributed under the terms of the Creative Commons Attribution License (CC-BY4.0), which permits any use, distribution and reproduction in any medium, provided the original author(s) and source are credited.

References

[1] F. Ares, S. Murciano and P. Calabrese, *Entanglement asymmetry as a probe of symmetry breaking*, *Nature Commun.* **14** (2023) 2036 [arXiv:2207.14693] [INSPIRE].

[2] L.K. Joshi et al., *Observing the quantum Mpemba effect in quantum simulations*, arXiv:2401.04270 [INSPIRE].

[3] C. Rylands et al., *Microscopic origin of the quantum Mpemba effect in integrable systems*, arXiv:2310.04419 [INSPIRE].

[4] S. Murciano, F. Ares, I. Klich and P. Calabrese, *Entanglement asymmetry and quantum Mpemba effect in the XY spin chain*, *J. Stat. Mech.* **2401** (2024) 013103 [arXiv:2310.07513] [INSPIRE].

[5] B. Bertini et al., *Dynamics of charge fluctuations from asymmetric initial states*, arXiv:2306.12404 [INSPIRE].

[6] F. Ferro, F. Ares and P. Calabrese, *Non-equilibrium entanglement asymmetry for discrete groups: the example of the XY spin chain*, *J. Stat. Mech.* **2402** (2024) 023101 [arXiv:2307.06902] [INSPIRE].

[7] F. Ares, S. Murciano, E. Vernier and P. Calabrese, *Lack of symmetry restoration after a quantum quench: an entanglement asymmetry study*, *SciPost Phys.* **15** (2023) 089 [arXiv:2302.03330] [INSPIRE].

[8] B.J.J. Khor et al., *Confinement and kink entanglement asymmetry on a quantum Ising chain*, arXiv:2312.08601 [INSPIRE].

[9] F. Ares, S. Murciano, L. Piroli and P. Calabrese, *An entanglement asymmetry study of black hole radiation*, arXiv:2311.12683 [INSPIRE].

[10] C. Holzhey, F. Larsen and F. Wilczek, *Geometric and renormalized entropy in conformal field theory*, *Nucl. Phys. B* **424** (1994) 443 [hep-th/9403108] [INSPIRE].

[11] P. Calabrese and J.L. Cardy, *Entanglement entropy and quantum field theory*, *J. Stat. Mech.* **0406** (2004) P06002 [hep-th/0405152] [INSPIRE].

[12] P. Calabrese and J. Cardy, *Entanglement entropy and conformal field theory*, *J. Phys. A* **42** (2009) 504005 [arXiv:0905.4013] [INSPIRE].

[13] L. Capizzi and V. Vitale, *A universal formula for the entanglement asymmetry of matrix product states*, arXiv:2310.01962 [INSPIRE].

[14] L. Capizzi and M. Mazzoni, *Entanglement asymmetry in the ordered phase of many-body systems: the Ising field theory*, *JHEP* **12** (2023) 144 [arXiv:2307.12127] [INSPIRE].

[15] M. Chen and H.-H. Chen, *Rényi entanglement asymmetry in $(1+1)$-dimensional conformal field theories*, *Phys. Rev. D* **109** (2024) 065009 [arXiv:2310.15480] [INSPIRE].

[16] J. Frohlich, J. Fuchs, I. Runkel and C. Schweigert, *Kramers-Wannier duality from conformal defects*, *Phys. Rev. Lett.* **93** (2004) 070601 [cond-mat/0404051] [INSPIRE].

[17] D. Gaiotto, A. Kapustin, N. Seiberg and B. Willett, *Generalized global symmetries*, *JHEP* **02** (2015) 172 [arXiv:1412.5148] [INSPIRE].

[18] M. Henkel and A. Patkós, *Conformal invariance and line defects in the two-dimensional Ising model*, *J. Phys. A* **21** (1988) L231.

[19] M. Henkel, A. Patkós and M. Schlottmann, *The Ising quantum chain with defects. 1. The exact solution*, *Nucl. Phys. B* **314** (1989) 609 [INSPIRE].

[20] L. Turban, *Conformal invariance and linear defects in the two-dimensional Ising model*, *J. Phys. A* **18** (1985) L325.

[21] F. Iglói, I. Peschel and L. Turban, *Inhomogeneous systems with unusual critical behaviour*, *Adv. Phys.* **42** (1993) 683.

[22] M. Oshikawa and I. Affleck, *Defect lines in the Ising model and boundary states on orbifolds*, *Phys. Rev. Lett.* **77** (1996) 2604 [hep-th/9606177] [INSPIRE].

[23] M. Oshikawa and I. Affleck, *Boundary conformal field theory approach to the critical two-dimensional Ising model with a defect line*, *Nucl. Phys. B* **495** (1997) 533 [cond-mat/9612187] [INSPIRE].

[24] V.B. Petkova and J.B. Zuber, *Generalized twisted partition functions*, *Phys. Lett. B* **504** (2001) 157 [hep-th/0011021] [INSPIRE].

[25] T. Quella, I. Runkel and G.M.T. Watts, *Reflection and transmission for conformal defects*, *JHEP* **04** (2007) 095 [hep-th/0611296] [INSPIRE].

[26] J. Frohlich, J. Fuchs, I. Runkel and C. Schweigert, *Duality and defects in rational conformal field theory*, *Nucl. Phys. B* **763** (2007) 354 [hep-th/0607247] [INSPIRE].

[27] P. Fendley, M.P.A. Fisher and C. Nayak, *Boundary conformal field theory and tunneling of edge quasiparticles in non-Abelian topological states*, *Annals Phys.* **324** (2009) 1547 [arXiv:0902.0998] [INSPIRE].

[28] C. Bachas, I. Brunner and D. Roggenkamp, *Fusion of critical defect lines in the 2D Ising model*, *J. Stat. Mech.* **1308** (2013) P08008 [arXiv:1303.3616] [INSPIRE].

[29] D. Aasen, R.S.K. Mong and P. Fendley, *Topological defects on the lattice I: the Ising model*, *J. Phys. A* **49** (2016) 354001 [arXiv:1601.07185] [INSPIRE].

[30] D. Aasen, P. Fendley and R.S.K. Mong, *Topological defects on the lattice: dualities and degeneracies*, arXiv:2008.08598 [INSPIRE].

[31] S. Murciano et al., *Measurement-altered Ising quantum criticality*, *Phys. Rev. X* **13** (2023) 041042 [arXiv:2302.04325] [INSPIRE].

[32] K. Sakai and Y. Satoh, *Entanglement through conformal interfaces*, *JHEP* **12** (2008) 001 [arXiv:0809.4548] [INSPIRE].

[33] V. Eisler and I. Peschel, *Entanglement in fermionic chains with interface defects*, *Annalen Phys.* **522** (2010) 679.

[34] P. Calabrese, M. Mintchev and E. Vicari, *Entanglement entropy of quantum wire junctions*, *J. Phys. A* **45** (2012) 105206 [arXiv:1110.5713] [INSPIRE].

[35] I. Peschel and V. Eisler, *Exact results for the entanglement across defects in critical chains*, *J. Phys. A* **45** (2012) 155301.

[36] E.M. Brehm and I. Brunner, *Entanglement entropy through conformal interfaces in the 2D Ising model*, *JHEP* **09** (2015) 080 [arXiv:1505.02647] [INSPIRE].

[37] M. Gutperle and J.D. Miller, *Entanglement entropy at CFT junctions*, *Phys. Rev. D* **95** (2017) 106008 [arXiv:1701.08856] [INSPIRE].

[38] M. Mintchev and E. Tonni, *Modular Hamiltonians for the massless Dirac field in the presence of a defect*, *JHEP* **03** (2021) 205 [arXiv:2012.01366] [INSPIRE].

[39] L. Capizzi, S. Murciano and P. Calabrese, *Rényi entropy and negativity for massless Dirac fermions at conformal interfaces and junctions*, *JHEP* **08** (2022) 171 [arXiv:2205.04722] [INSPIRE].

[40] L. Capizzi, S. Murciano and P. Calabrese, *Full counting statistics and symmetry resolved entanglement for free conformal theories with interface defects*, *J. Stat. Mech.* **2307** (2023) 073102 [arXiv:2302.08209] [INSPIRE].

[41] L. Capizzi and A. Rotaru, *Thermal entanglement in conformal junctions*, arXiv:2312.08275 [INSPIRE].

[42] Z. Yang, D. Mao and C.-M. Jian, *Entanglement in a one-dimensional critical state after measurements*, *Phys. Rev. B* **108** (2023) 165120 [arXiv:2301.08255] [INSPIRE].

[43] Z. Weinstein, R. Sajith, E. Altman and S.J. Garratt, *Nonlocality and entanglement in measured critical quantum Ising chains*, *Phys. Rev. B* **107** (2023) 245132 [arXiv:2301.08268] [INSPIRE].

[44] J.Y. Lee, C.-M. Jian and C. Xu, *Quantum criticality under decoherence or weak measurement*, *PRX Quantum* **4** (2023) 030317 [arXiv:2301.05238] [INSPIRE].

[45] Y. Ashida, S. Furukawa and M. Oshikawa, *System-environment entanglement phase transitions*, arXiv:2311.16343 [INSPIRE].

[46] P. Ruggiero, P. Calabrese, T. Giamarchi and L. Foini, *Electrostatic solution of massless quenches in Luttinger liquids*, *SciPost Phys.* **13** (2022) 111 [arXiv:2203.06740] [INSPIRE].

[47] M. Goldstein and E. Sela, *Symmetry-resolved entanglement in many-body systems*, *Phys. Rev. Lett.* **120** (2018) 200602 [arXiv:1711.09418] [INSPIRE].

[48] J.C. Xavier, F.C. Alcaraz and G. Sierra, *Equipartition of the entanglement entropy*, *Phys. Rev. B* **98** (2018) 041106 [arXiv:1804.06357] [INSPIRE].

[49] R. Bonsignori, P. Ruggiero and P. Calabrese, *Symmetry resolved entanglement in free fermionic systems*, *J. Phys. A* **52** (2019) 475302 [arXiv:1907.02084] [INSPIRE].

[50] E. Cornfeld, M. Goldstein and E. Sela, *Imbalance entanglement: symmetry decomposition of negativity*, *Phys. Rev. A* **98** (2018) 032302 [arXiv:1804.00632] [INSPIRE].

[51] S. Murciano, G. Di Giulio and P. Calabrese, *Entanglement and symmetry resolution in two dimensional free quantum field theories*, *JHEP* **08** (2020) 073 [arXiv:2006.09069] [INSPIRE].

[52] P. Calabrese, J. Dubail and S. Murciano, *Symmetry-resolved entanglement entropy in Wess-Zumino-Witten models*, *JHEP* **10** (2021) 067 [arXiv:2106.15946] [INSPIRE].

[53] L. Capizzi, P. Ruggiero and P. Calabrese, *Symmetry resolved entanglement entropy of excited states in a CFT*, *J. Stat. Mech.* **2007** (2020) 073101 [arXiv:2003.04670] [INSPIRE].

[54] H.-H. Chen, *Symmetry decomposition of relative entropies in conformal field theory*, *JHEP* **07** (2021) 084 [arXiv:2104.03102] [INSPIRE].

[55] L. Capizzi and P. Calabrese, *Symmetry resolved relative entropies and distances in conformal field theory*, *JHEP* **10** (2021) 195 [arXiv:2105.08596] [INSPIRE].

[56] R. Bonsignori and P. Calabrese, *Boundary effects on symmetry resolved entanglement*, *J. Phys. A* **54** (2021) 015005 [arXiv:2009.08508] [INSPIRE].

[57] B. Estienne, Y. Ikhlef and A. Morin-Duchesne, *Finite-size corrections in critical symmetry-resolved entanglement*, *SciPost Phys.* **10** (2021) 054 [arXiv:2010.10515] [INSPIRE].

[58] S. Murciano, R. Bonsignori and P. Calabrese, *Symmetry decomposition of negativity of massless free fermions*, *SciPost Phys.* **10** (2021) 111 [arXiv:2102.10054] [INSPIRE].

[59] A. Milekhin and A. Tajdini, *Charge fluctuation entropy of Hawking radiation: a replica-free way to find large entropy*, *SciPost Phys.* **14** (2023) 172 [arXiv:2109.03841] [INSPIRE].

[60] F. Ares, P. Calabrese, G. Di Giulio and S. Murciano, *Multi-charged moments of two intervals in conformal field theory*, *JHEP* **09** (2022) 051 [arXiv:2206.01534] [INSPIRE].

[61] H.-H. Chen, *Charged Rényi negativity of massless free bosons*, *JHEP* **02** (2022) 117 [arXiv:2111.11028] [INSPIRE].

[62] M. Ghasemi, *Universal thermal corrections to symmetry-resolved entanglement entropy and full counting statistics*, *JHEP* **05** (2023) 209 [arXiv:2203.06708] [INSPIRE].

[63] M. Fossati, F. Ares and P. Calabrese, *Symmetry-resolved entanglement in critical non-Hermitian systems*, *Phys. Rev. B* **107** (2023) 205153 [arXiv:2303.05232] [INSPIRE].

[64] H. Gaur and U.A. Yajnik, *Charge imbalance resolved Rényi negativity for free compact boson: two disjoint interval case*, *JHEP* **02** (2023) 118 [arXiv:2210.06743] [INSPIRE].

[65] G. Di Giulio et al., *On the boundary conformal field theory approach to symmetry-resolved entanglement*, *SciPost Phys. Core* **6** (2023) 049 [arXiv:2212.09767] [INSPIRE].

[66] A. Foligno, S. Murciano and P. Calabrese, *Entanglement resolution of free Dirac fermions on a torus*, *JHEP* **03** (2023) 096 [arXiv:2212.07261] [INSPIRE].

[67] C. Northe, *Entanglement resolution with respect to conformal symmetry*, *Phys. Rev. Lett.* **131** (2023) 151601 [arXiv:2303.07724] [INSPIRE].

[68] Y. Kusuki, S. Murciano, H. Ooguri and S. Pal, *Symmetry-resolved entanglement entropy, spectra & boundary conformal field theory*, *JHEP* **11** (2023) 216 [arXiv:2309.03287] [INSPIRE].

[69] A. Bruno, F. Ares, S. Murciano and P. Calabrese, *Symmetry resolution of the computable cross-norm negativity of two disjoint intervals in the massless Dirac field theory*, *JHEP* **02** (2024) 009 [arXiv:2312.02926] [INSPIRE].

[70] L. Bhardwaj et al., *Lectures on generalized symmetries*, *Phys. Rept.* **1051** (2024) 1 [arXiv:2307.07547] [INSPIRE].

[71] M.A. Nielsen and I.L. Chuang, *Quantum computation and quantum information:* 10th *anniversary edition*, Cambridge University Press, Cambridge, U.K. (2010) [DOI:10.1017/cbo9780511976667] [INSPIRE].

[72] Z. Ma, C. Han, Y. Meir and E. Sela, *Symmetric inseparability and number entanglement in charge-conserving mixed states*, *Phys. Rev. A* **105** (2022) 042416 [arXiv:2110.09388] [INSPIRE].

[73] J.L. Cardy and I. Peschel, *Finite size dependence of the free energy in two-dimensional critical systems*, *Nucl. Phys. B* **300** (1988) 377 [INSPIRE].

[74] J.-M. Stéphan and J. Dubail, *Logarithmic corrections to the free energy from sharp corners with angle* 2π, *J. Stat. Mech.* **1309** (2013) P09002 [arXiv:1303.3633] [INSPIRE].

[75] J.-M. Stéphan, *Emptiness formation probability, Toeplitz determinants, and conformal field theory*, *J. Stat. Mech.* **2014** (2014) P05010 [arXiv:1303.5499].

[76] A. Lamacraft and P. Fendley, *Order parameter statistics in the critical quantum Ising chain*, *Phys. Rev. Lett.* **100** (2008) 165706 [arXiv:0802.1246] [INSPIRE].

[77] P. Di Francesco, P. Mathieu and D. Senechal, *Conformal field theory*, Springer-Verlag, New York, NY, U.S.A. (1997) [DOI:10.1007/978-1-4612-2256-9] [INSPIRE].

[78] R.W. Cherng and E. Demler, *Quantum noise analysis of spin systems realized with cold atoms*, *New J. Phys.* **9** (2007) 7.

[79] S. Groha, F. Essler and P. Calabrese, *Full counting statistics in the transverse field Ising chain*, *SciPost Phys.* **4** (2018) 043.

[80] D.A. Ivanov and A.G. Abanov, *Characterizing correlations with full counting statistics: classical Ising and quantum XY spin chains*, *Phys. Rev. E* **87** (2013) 022114.

[81] F. Ares, M.A. Rajabpour and J. Viti, *Exact full counting statistics for the staggered magnetization and the domain walls in the XY spin chain*, *Phys. Rev. E* **103** (2021) 042107 [arXiv:2012.14012] [INSPIRE].

[82] C.-M. Chang et al., *Topological defect lines and renormalization group flows in two dimensions*, *JHEP* **01** (2019) 026 [arXiv:1802.04445] [INSPIRE].

[83] L. Bhardwaj and Y. Tachikawa, *On finite symmetries and their gauging in two dimensions*, *JHEP* **03** (2018) 189 [arXiv:1704.02330] [INSPIRE].

[84] E.H. Lieb, T. Schultz and D. Mattis, *Two soluble models of an antiferromagnetic chain*, *Annals Phys.* **16** (1961) 407 [INSPIRE].

[85] I. Peschel, *Calculation of reduced density matrices from correlation functions*, *J. Phys. A* **36** (2003) L205 [cond-mat/0212631] [INSPIRE].